

Evolution of Ossoue Glacier (French Pyrenees) since the end of the Little Ice Age

R. Marti et al.

Evolution of Ossoue Glacier (French Pyrenees) since the end of the Little Ice Age

R. Marti^{1,2}, S. Gascoïn², T. Houet¹, O. Ribière¹, D. Laffly¹, T. Condom³, S. Monnier⁴, M. Schmutz⁵, C. Camerlynck⁶, J. P. Tihay⁷, J. M. Soubeyroux⁸, and P. René⁹

¹Géographie de l'Environnement (GEODE), Toulouse, France

²Centre d'Etudes Spatiales de la Biosphère (CESBIO), Toulouse, France

³Laboratoire d'étude des Transferts en Hydrologie et Environnement (LTHE), Université Grenoble-Alpes, Grenoble, France

⁴Instituto de Geografia, Pontificia Universidad Católica de Valparaíso, Chile

⁵Institut Polytechnique de Bordeaux (IPD), Pessac, France

⁶Structure et fonctionnement des systèmes hydriques continentaux (SISYPHE), Université Pierre et Marie Curie, Paris VI, France

⁷Université de Pau et des Pays de l'Adour (UPPA), Pau, France

⁸Météo France, Direction de la Climatologie (DCLIM), Toulouse, France

⁹Association MORAINÉ, Luchon, France

Title Page	
Abstract	Introduction
Conclusions	References
Tables	Figures
◀	▶
◀	▶
Back	Close
Full Screen / Esc	
Printer-friendly Version	
Interactive Discussion	



Received: 6 February 2015 – Accepted: 20 March 2015 – Published: 17 April 2015

Correspondence to: R. Marti (renaud.marti@gmail.com)

Published by Copernicus Publications on behalf of the European Geosciences Union.

TCD

9, 2431–2494, 2015

Evolution of Ossoue Glacier (French Pyrenees) since the end of the Little Ice Age

R. Marti et al.

Title Page

Abstract

Introduction

Conclusions

References

Tables

Figures



Back

Close

Full Screen / Esc

Printer-friendly Version

Interactive Discussion

Abstract

Long-term climate records are rare at high elevations in Southern Europe. Here, we reconstructed the evolution of Ossoue Glacier (42°46' N, 0.45 km²), located in the Pyrenees (3404 m a.s.l.), since the Little Ice Age (LIA). Glacier length, area, thickness and mass changes indicators were generated from historical datasets, topographic surveys, glaciological measurements (2001–2013), a GPR survey (2006) and stereoscopic satellite images (2013). The glacier has receded considerably since the end of the LIA, losing 40 % of its length and 60 % of its area. Three periods of marked ice depletion can be identified: 1850–1890, 1928–1950 and 1983–2013, as well as two periods of stabilization or slightly growth: 1905–1928 and 1950–1983; these agree with climatic datasets (air temperature, precipitation, North Atlantic Oscillation, Atlantic Multidecadal Oscillation). In the early 2000s, the area of the glacier dropped below 50 % of its area at the end of the LIA. Geodetic mass balance measurements over 1983–2013 indicated -30.1 ± 1.7 m w.e. (-1 m w.e. yr⁻¹) whereas glaciological mass balance measurements show -17.36 ± 2.9 m w.e. (-1.45 m w.e. yr⁻¹) over 2001–2013, resulting in a doubling of the ablation rate in the last decade. In 2013 the maximum ice thickness was 59 ± 10.3 m. Assuming that the current ablation rate stays constant, Ossoue Glacier will disappear midway through the 21st century.

1 Introduction

Southern Europe is projected to be a hotspot of climate change over the 21st century, with increasing temperatures and decreasing precipitation (IPCC, 2013). Among other consequences, water resources, including snowmelt from mountain areas, could be affected while water demand should will likely increase (EEA, 2012; IPCC, 2013).

The Pyrenees are a mountain range in southwestern Europe spanning ~ 430 km from the Bay of Biscay (Atlantic Ocean) to the Mediterranean Sea. According to regional climate model projections, the thickness and duration of its snowpack could de-

TCD

9, 2431–2494, 2015

Evolution of Ossoue Glacier (French Pyrenees) since the end of the Little Ice Age

R. Marti et al.

Title Page

Abstract

Introduction

Conclusions

References

Tables

Figures

◀

▶

◀

▶

Back

Close

Full Screen / Esc

Printer-friendly Version

Interactive Discussion



Evolution of Ossoue Glacier (French Pyrenees) since the end of the Little Ice Age

R. Marti et al.

Title Page

Abstract

Introduction

Conclusions

References

Tables

Figures

◀

▶

◀

▶

Back

Close

Full Screen / Esc

Printer-friendly Version

Interactive Discussion

cline over the 21st century (López-Moreno et al., 2009). However, analysis of snow depth observations over 1985–1999 in the Spanish Pyrenees showed contrasting trends, with increasing snow depth above 2200 m elevation and decreasing snow depth below 2200 m (López-Moreno, 2005). Tree-ring time series from living trees and in situ relict samples, collected at elevations of 2200–2450 m a.s.l., have allowed the reconstruction of 1260–2005 summer temperatures in the Pyrenees. The data confirmed the twentieth century warming (Büntgen et al., 2008). The longest meteorological time series in the French Pyrenees began in 1882 at an astronomical observatory located on the Pic du Midi (2862 m a.s.l.). A mean annual temperature increase of 0.83 °C has been observed over 1882–1970 with a significant decrease in the mean annual diurnal temperature range (2.89 °C per century) (Bücher and Dessens, 1991; Dessens and Bücher, 1995). Recent work on data homogenization within the framework of the Pyrenean Climate Change Observatory depicts a uniform warming at the massif scale over the last sixty years, and highlights a significant warming signal from the 1980s (Soubeyroux et al., 2011; Camberlin and Yves, 2014)

Due to the paucity of meteorological measurements, Pyrenean climate proxy records are crucial to reconstruct past climate fluctuations at secular scales and high altitudes. Glaciers are considered robust climate proxies (WGMS, 2008; Zemp et al., 2009). The Pyrenees hosts the European southernmost glaciers in Europe, all below the 43° N latitude. Their small sizes (< 1 km²), relatively low elevations, and southern locations make them particularly vulnerable to climate warming (Grunewald and Scheithauer, 2010). Pyrenean glaciers are strongly out of balance with regional climate and are retreating quickly (Chueca et al., 2007).

The Ossoue Glacier (42°46′ N, 0.45 km²) is the second largest glacier in the Pyrenees. In comparison with that of other pyrenean glaciers, the evolution of Ossoue Glacier is well documented, with observations starting at the end of the 19th century. These include historical datasets, topographic maps, aerial images and stakes measurements. The objective of this paper is to reconstruct the evolution of Ossoue Glacier

based on these data to provide further information on the Pyrenean climate since the end of the Little Ice Age (LIA).

The first section gives a brief review of glaciers studies in the Pyrenees (Sect. 2). After describing the site of Ossoue Glacier (Sect. 3), we propose a reconstruction of various indicators including glacier length, area and mass balance of Ossoue Glacier (Sects. 4 and 5). We use ground penetrating radar (GPR) measurements collected in 2006 to estimate the ice depth in the upper part of the glacier. The combination of these indicators allows us to depict a consistent evolution of the glacier since the LIA for the first time. Finally, we discuss the response of the glacier to past climatic changes (temperature, precipitation) and a possible connection with the North Atlantic Oscillation (NAO) and the Atlantic Multidecadal Oscillation (AMO) (Sect. 6).

2 Glaciers studies in the Pyrenees

The last favorable period to glacier development in the Pyrenees was the Little Ice Age (LIA), which occurred between the 14th and 19th centuries (Grove, 2004). LIA climate cooling in the Pyrenees led to the formation and advance of glaciers in fifteen massifs where there are up to one hundred cirques (Trueba et al., 2008). In the middle of the 19th century, after advance and recession phases, the Pyrenean glacier fronts reached positions close to their maximum LIA extent. At that time, the area of Pyrenean glaciers is estimated to be slightly over 20 km² (Chueca et al., 2007). Since then, their area covered 8 km² in 1984 (Serrat-Ventura, 1988), 6 km² in 2004 (Chueca et al., 2004) and approximately 3 km² in 2013 (René, 2014).

Due to their remote locations and small sizes, Pyrenean glaciers have not benefited from long-term glaciological studies (Grove, 2004). Early topographic measurements were made by “Pyreneists”, alpinists who became enthusiasts in the exploration and observation of the Pyrenees (de Carbonnières, 1801; von Charpentier, 1823; Trutat Eugène, 1876; Schrader, 1895). The *Commission Internationale des Glaciers* (CIG) was created in 1894 in Zürich and led thereafter to the present-day International Asso-

Evolution of Ossoue Glacier (French Pyrenees) since the end of the Little Ice Age

R. Marti et al.

Title Page

Abstract

Introduction

Conclusions

References

Tables

Figures

◀

▶

◀

▶

Back

Close

Full Screen / Esc

Printer-friendly Version

Interactive Discussion



Evolution of Ossoue Glacier (French Pyrenees) since the end of the Little Ice Age

R. Marti et al.

Title Page

Abstract

Introduction

Conclusions

References

Tables

Figures

◀

▶

◀

▶

Back

Close

Full Screen / Esc

Printer-friendly Version

Interactive Discussion

ciation of Cryospheric Sciences (IACS) (Radok, 1997; Jones, 2008). Its first president, the Swiss François-Alphonse Forel, promoted the organized monitoring of glaciers in the Pyrenees for comparison to the evolution of the glaciers in the Alps (Forel, 1887; Gellatly et al., 1994). Prince Roland Bonaparte established and communicated to the Commission the first regular observations of glacier frontal variations between 1874 and 1895 (Bonaparte, 1892). Next, Gaurier monitored the glaciers over the period 1904–1927, which was interrupted by World War I (Gaurier, 1921). On the French side of the Pyrenees, *Eaux et Forêts*, the French national agency in charge of forest and water management, took over the measurements in year 1932, and after World War II, during the period 1945–1956 (Mercanton, 1956). At the end of the 1970s, under the initiative of François Valla from the *Centre Technique du Génie Rural et des Eaux et Fôrets* and the support of the *Parc National des Pyrénées*, the first mass balance measurements in the Pyrenees to our knowledge were performed at Ossoue Glacier between 1978 and 1984 (with only qualitative data taken in 1983 and 1984) (Pont and Valla, 1980; Pont, 1985). This initiative led to the creation of the *Groupe d'Etudes des Glaciers des Pyrénées* (GEGP), a collaborative group comprising the *Institut National de l'Information Géographique et Forestière* (IGN) and researchers at Pau University. Two topographic maps dated from 1948 and 1983 and shown below were produced by the GEGP (Cazenave-Piarrot et al., 1987). However, this group lasted only a few years, so that between 1957 and 2001, only raw terrestrial and aerial images are available for reconstructing glacier front and area variations. Since 2001, a group of volunteer glaciologists called the *Association Moraine* have performed regular glaciological field measurements (René, 2014). On the Spanish side, the institutional program *Evaluación de Recursos Hídricos Procedentes de Innivación* (EHRIN) has monitored Spanish glaciers since the 1990s. Since 1991, this program has collected an uninterrupted glaciological mass balance time series of the Maladeta Glacier (still ongoing WGMS, 2008). The ablation stake measurement protocol in Spain and France was established in collaboration with glaciologists from the *Laboratoire de Glaciologie et Géophysique*

de l'Environnement (Grenoble, France), which facilitates comparison between glaciers fluctuations in the Pyrenees and Alps.

In spite of all these efforts, observations of the Pyrenean glaciers remain scarce and irregular. Hence, there are few available reconstructions of glacier evolution since the LIA, and quantitative studies are even rarer. A brief review of Pyrenean glacier evolution is given in Chueca and Julian (2004). On the Spanish side of the Pyrenees, the ice-covered area decreased by 74 % since the end of the LIA (Chueca et al., 2008). In comparison, the area of glaciers in the European Alps decreased by 35 % (Hoelzle et al., 2007). Field measurements completed by early maps, paintings, terrestrial and aerials photographs have allowed the reconstruction of the fluctuations of the Tailon, Maladeta and Coronas Glaciers throughout the 20th century (Gellatly et al., 1994; Chueca et al., 2003; Cía et al., 2005; Chueca et al., 2007). The results of these studies are consistent with a general glacier recession since the LIA. Each glacier experienced alternating periods of strong recession and periods of stability or limited readvance. In particular, there seems to be a common period of strong recession after 1850, a period of readvance or stability between 1960 and 1980, and a period of strong recession from the mid-1980s until now.

The main driver of these glacier changes since the LIA is the regional temperature increase (Grunewald and Scheithauer, 2010). Periods of low precipitation were identified without evident trends. Investigation into potential connections to larger-scale atmospheric patterns has been less common. The NAO controlled the snow accumulation in the Pyrenees during the second half of the 20th century, in particular at high-elevation (López-Moreno et al., 2007, 2011). The AMO was more recently identified as a possible driver of multi-decadal variations in river flow and precipitation in southwest France including the Pyrenees (Giuntoli et al., 2013; Boé and Habets, 2014).

Local topo-climatic effects such as avalanching, wind-drifted snow or shading may significantly influence accumulation and ablation processes. In the Pyrenees, these local influences are expected to have introduced spatial disparities in ice shrinkage,

TCD

9, 2431–2494, 2015

Evolution of Ossoue Glacier (French Pyrenees) since the end of the Little Ice Age

R. Marti et al.

Title Page

Abstract

Introduction

Conclusions

References

Tables

Figures

◀

▶

◀

▶

Back

Close

Full Screen / Esc

Printer-friendly Version

Interactive Discussion

2011). The melting period extends generally from the end of May to the beginning of October. We thus consider the hydrological summer (JJAS). Moulins are often observed during that period in the glacier upper area.

Ossoue Glacier was irregularly monitored throughout the 20th century, but has been quite well monitored since 2001 (Tab. 2).

4 Data sets and methods

4.1 Topographic surveys

4.1.1 Early sources

As is usual in glacier reconstructions, our data come from various sources (Tab. 2). Distances between the glacier snout and reference points (spits, marks) on specific dates were measured in situ or from photographs or aerial images. Moraines allow us to determine the glacier extent at dates estimated to be close to the end the LIA. The testimony of Henri Passet establishes that the glacier reached the summit of the left lateral moraine in 1865 (Grove, 2004). A photograph taken in 1885 by Joseph Vallot provides evidence that Ossoue Glacier was still close to its moraines at this date. The Etat-Major map edited in 1851 by the French army also provides similar evidence. The map has an estimated accuracy of 15 m in planimetry. Two elevation points located on the front of the glacier are marked at 2458 and 2471 m a.s.l. Currently, both points are located on the glacier moraine. At these locations, the present elevations are 2447 and 2491 m a.s.l. It is remarkable that the difference in elevations are only 11 and 20 m, which gives us further confidence in the fact that the glacier front was actually in contact with its moraine at the middle of the 19th century, i.e., at the estimated end of the LIA in the Pyrenees (Grove, 2004; Trueba et al., 2008).

Evolution of Ossoue Glacier (French Pyrenees) since the end of the Little Ice Age

R. Marti et al.

Title Page

Abstract

Introduction

Conclusions

References

Tables

Figures

◀

▶

◀

▶

Back

Close

Full Screen / Esc

Printer-friendly Version

Interactive Discussion



The Villa Russell is a cave accessible from the glacier at 3201 m a.s.l. It was extruded by Henry Russell and his employees in 1881 (Fig. 4, Tab. 2). Vertical measurements between the glacier surface and the cave threshold were made beginning in 1882.

We collected three paper topographic maps from 1924, 1948 and 1983 (Fig. 5 and Tab. 2). The map dated from 1924 is a 1 : 20 000 scale topographic map with 20 m contour lines. It was created by Alphonse Meillon, a pyrenean topograph-alpinist from the *Club Alpin Français* and Etienne de Larminat, a military cartographer (Meillon and de Larminat, 1933). Its implementation involved both field measurements and triangulation from photographs. Most of the photographs were terrestrial photographs, but military aerial photographs were also used to fill the gaps in a unique collaboration framework (Guilhot, 2005). The maps from 1948 and 1983 feature 2 m contour lines maps and were drafted by GEGP (Sect. 2). Elevation contour lines were generated by manual restitution from stereoscopic airborne photographs (Cazenave-Piarrot et al., 1987). Both maps have a 1 : 2500 scale and were projected in Lambert 3 (the official French coordinate projection system until 2001). We digitized these maps at 1270 dpi.

We also collected summer aerial photographs dated from 1924, 1948 and 1983 available in the IGN in digital format. The latter two photographs exhibit crevasses features matching the aforementioned topographic maps, which indicates that they were used as stereoscopic images to generate the contour lines. We used these photographs to delineate the glacier outline and compute the glacier area, because we found that the glacier outline on the topographic maps was either incomplete or inaccurate. We also used the Etat-Major map (dated 1851) to compute the glacier area. We preferred the outline derived from the moraine position to that from this map to determine the glacier outline in and around the 1850s.

Orthorectification, photointerpreation, length and area measurements (based on graphical or digital sources) were performed in GIS (ArcGis 10.2 from Esri®).

Because there was no projection information available for 1924, the map was georeferenced by extracting GCPs from a digital reference map at 1 : 25 000 scale (IGN Scan 25). For the 1948 and 1983 maps, the coordinates of the graticule intersections

Evolution of Ossoue Glacier (French Pyrenees) since the end of the Little Ice Age

R. Marti et al.

Title Page

Abstract

Introduction

Conclusions

References

Tables

Figures

◀

▶

◀

▶

Back

Close

Full Screen / Esc

Printer-friendly Version

Interactive Discussion



Evolution of Ossoue Glacier (French Pyrenees) since the end of the Little Ice Age

R. Marti et al.

Title Page

Abstract

Introduction

Conclusions

References

Tables

Figures

◀

▶

◀

▶

Back

Close

Full Screen / Esc

Printer-friendly Version

Interactive Discussion



To complete the historic DEMs time series, two DGPS surveys (DGPS receivers Trimble GEO XH 2008 and 6000) were performed on 3 September 2011 and 6 October 2013 (Tab. 2). Post-corrections based on a 40-km-distant base from the French geodetic permanent network (RGP) were applied. Two m DEMs were generated from the elevation point canvas applying the same interpolation method previously mentioned. The estimated random error on the DGPS DEM is 0.6 m.

A Pléiades stereo pair was acquired over Ossoue Glacier on 23 September 2013. We generated a 2 m horizontal resolution DEM with 1 m vertical resolution and 1.8 m vertical accuracy (GeoView©software 6.6, Marti et al., 2014). In this study, the Pléiades DEM was used to generate the surface elevation of the deglaciated margin between 1983 and 2013. To map the differences in surface elevation on the glacier between 1983 and 2013, the DGPS surface elevation was used because it was acquired closer to the end of the summer.

4.2 Geodetic mass balances

The DEMs generated for 1924, 1948, 1983, 2011 and 2013 allowed us to establish a geodetic mass balance over an 89 year period. Consecutive DEMs were subtracted on a pixel by pixel basis. Volume changes derived by differencing DEMs is based on the following equation (Zemp et al., 2013):

$$\Delta V = r^2 \sum_{k=1}^K \Delta h_k \quad (2)$$

where K is the number of pixels covering the glacier at the maximum extent, Δh_k is the elevation difference at pixel k , and r is the pixel size (2 m in this study).

We have very little information on the generation of the maps based on terrestrial (1924) or aerial photogrammetry (1948, 1983). DEMs were assessed on stable terrain following the technical recommendations given in Racoviteanu et al. (2010). A GCPs dataset was generated from DGPS points collected on 23 October 2013 on the frontal

margin of the glacier, i.e., on a snow and ice free bedrock surface. DEMs were not horizontally shifted given the good absolute localization of the sources (5 m for 1924, 2 m for 1948 and 1983), and the limited superficies covered outside the glacier to perform such an adjustment.

The differences between the DEM and the DGPS elevation values were normally distributed for 1948, 1983 and 2013. The mean elevation difference found for each DEM was noted as e_{bias} ($e_{\text{bias.1948}} = -1.8$ m, $e_{\text{bias.1983}} = -1.4$ m, and $e_{\text{bias.2013.P}} = -1.37$ m for the 2013 Pléiades DEM) and was uniformly added to all the elevation values. For the 1924 DEM, the elevation differences did not follow a normal distribution and it was not possible to determine the elevation bias (noted as $e_{\text{bias.1924}}$). Hence, no correction was applied to this DEM. The SD of the elevation difference values on stable areas was considered as to be a representative value of the vertical random error and was noted as σ_{bias} . The random error term due to the interpolation process was calculated to be 0.5 m for 2011 and 2013 DGPS data. The geodetic mass balance B_{geod} was calculated through the following formula:

$$B_{\text{geod}} = \rho \left(\frac{\Delta V_{\text{gla}}}{A_{\text{gla}}} + \frac{\Delta V_{\text{marg.gain}}}{A_{\text{marg.gain}}} + \frac{\Delta V_{\text{marg.loss}}}{A_{\text{marg.loss}}} \right) \quad (3)$$

where ρ is the mean density (see detail below). A_{gla} is the area that is glaciated in both DEMs. $A_{\text{marg.loss}}$ is the deglaciated area; $A_{\text{marg.gain}}$ is the area where the glacier advanced. The mean density was assumed to be 900 kg m^{-3} between 1924 and 1948, and between 1983 and 2013, because the firn zone was nearly absent during those periods. We neglected the errors associated with this density assumption. In 1983, because a firn zone was likely present, we used a mean density of 850 kg m^{-3} with an uncertainty range of $\pm 50 \text{ kg m}^{-3}$ (Huss, 2013). For that period, we calculated an error term σ_{dc} associated with the uncertainty range due to density conversion. For every period, we considered an additional systematic error term e_t due to the time lag between the raw data acquisition date and the first day of the next hydrological year, fixed to 1 October (when the elevation surface is expected to reach its annual minimum).

Evolution of Ossoue Glacier (French Pyrenees) since the end of the Little Ice Age

R. Marti et al.

Title Page

Abstract

Introduction

Conclusions

References

Tables

Figures

◀

▶

◀

▶

Back

Close

Full Screen / Esc

Printer-friendly Version

Interactive Discussion



The error ϵ_t was computed by multiplying the mean ablation rate observed during this period of the year over 2001–2013 (from stake measurements) by the duration of the time lag. At this stage we preferred to keep this term as an error rather than correcting the mass balance value, using a floating-date system (Cogley et al., 2011).

Following Zemp et al. (2013) the mean annual systematic error may be expressed as:

$$\overline{\epsilon_{\text{geod.total.a}}} = \frac{\epsilon_{\text{geod.total.PoR}}}{N} = \frac{\epsilon_{\text{geod.DEM.PoR}}}{N} \quad (4)$$

$$= \frac{\epsilon_{\text{bias}} + \epsilon_t}{N} \quad (5)$$

where PoR is period of record and N is the number of years in the PoR. After co-registration ϵ_{bias} is assumed to be 0, and therefore:

$$\overline{\epsilon_{\text{geod.total.a}}} = \frac{\epsilon_t}{N} \quad (6)$$

The mean annual random error may be expressed following (Zemp et al., 2013):

$$\overline{\sigma_{\text{geod.total.a}}} = \frac{\sigma_{\text{geod.total.PoR}}}{N} = \frac{\sqrt{\sigma_{\text{geod.DEM.PoR}}^2}}{N} \quad (7)$$

$$= \frac{\sqrt{\sigma_{\text{bias}}^2 + \sigma_{\text{dc}}^2}}{N} \quad (8)$$

Note that for scaling random errors at annual time steps, division is by the number of years (Zemp et al., 2013). The values of ϵ_{bias} , ϵ_t , σ_{bias} , σ_{dc} and the resulting errors in DEM differences are given in Table 3. Annualized systematic and random errors are presented in Table 10.

Evolution of Ossoue Glacier (French Pyrenees) since the end of the Little Ice Age

R. Marti et al.

Title Page

Abstract

Introduction

Conclusions

References

Tables

Figures

◀

▶

◀

▶

Back

Close

Full Screen / Esc

Printer-friendly Version

Interactive Discussion



4.3 Glaciological mass balances

Since 2001, Ossoue Glacier has been monitored by systematic winter and summer mass balance measurements performed by Association Moraine. These are available on the WGMS website (Id: 2867). The direct glaciological method was used here (Ostrem-Brugman, 1991; Cuffey and Paterson, 2010). The protocol was similar to that used for Saint-Sorlin and Argentière Glaciers in the Alps (Gerbaux et al., 2005; Vincent, 2002) and followed the technical recommendations of the GLACIOCLIM observation network (GLACIOCLIM, 2001; René, 2013). At eight sites (Fig. 4), the winter and annual mass balances were determined by two specific methods: (1) the end of winter snow depth with respect to the previous summer surface was measured using snow probes and the near-surface snow density was calculated by drilling and weighting calibrated cores; and (2) the annual mass balance was determined by inserting 10 m ablation stakes (five 2 m sections) into the ice. Summer ablation measurements were repeated once a month until a date close to the beginning of the next hydrological year, according to the floating-date system (Cogley et al., 2011).

These point observations were spatially integrated using an area extrapolation method. The glacier surface was divided into eight polygons centered at each ablation stake. The polygon borders were determined through empirical considerations based on field observations, elevation, aspect and mean slope (Tab. 4, Fig. 4). The winter mass balance at a specific site k can be expressed as:

$$b_{w,k} = \rho_{\text{snow},k} h_{\text{snow},k} \quad (9)$$

where $\rho_{\text{snow},k}$ is the density calculated at site k and $h_{\text{snow},k}$ the snow depth accumulated during winter on the previous summer surface.

The glacier-wide winter mass balance B_w was obtained by summing the contribution from each polygon:

$$B_w = \sum_k b_{w,k} W_k \quad (10)$$

TCO

9, 2431–2494, 2015

Evolution of Ossoue Glacier (French Pyrenees) since the end of the Little Ice Age

R. Marti et al.

Title Page

Abstract

Introduction

Conclusions

References

Tables

Figures

◀

▶

◀

▶

Back

Close

Full Screen / Esc

Printer-friendly Version

Interactive Discussion



where W_k is the fractional surface area of the polygon k within the glacier (Tab. 4). The W_k values were updated in 2006 and 2011 to reflect the evolution of the glacier geometry.

The annual mass balance was calculated using the same spatial integration method.

If the field operator noted the disappearance of the winter snow layer, and the presence of older firn from a previous year, a density of 600 kg m^{-3} was applied to that layer. If ice was observed, a constant density $\rho_{\text{ice}} = 900 \text{ kg m}^{-3}$ was used. Lower densities values were not used because of the continuous glacier shrinkage observed since the 1980s.

These glaciological mass balance terms can be expressed in the following equation (Cogley et al., 2011):

$$B_{\text{glac.a}} = B_w + B_s \quad (11)$$

where $B_{\text{glac.a}}$, B_w and B_s designate the glacier-wide annual, winter and summer mass balances, respectively.

The summer balance B_s was calculated as the difference between the two measured mass balance terms.

Annual systematic and random errors in the glaciological data series can be expressed as follows (Zemp et al., 2013):

$$\overline{\epsilon}_{\text{glac.total.a}} = \frac{\epsilon_{\text{glac.PoR}}}{N} \quad (12)$$

$$\overline{\sigma}_{\text{glac.total.a}} = \frac{\sum_{t=1}^N \sigma_{\text{glac.a.PoR}}}{\sqrt{N}} = \frac{\sqrt{\sum_{t=1}^N \sigma_{\text{glac.point.t}}^2 + \sigma_{\text{glac.spatial.t}}^2 + \sigma_{\text{glac.ref.t}}^2}}{\sqrt{N}} \quad (13)$$

where PoR indicates the period of record, N is number of years in the PoR and point refers to the field measurement at the location point, spatial to spatial integration, and ref to the changing glacier area over time.

The value of $\overline{\epsilon}_{\text{glac.total.a}}$ was computed from the DPGS surveys performed in 2006 and 2011 as follows: (i) we calculated the mean elevation difference between both DEMs

Evolution of Ossoue Glacier (French Pyrenees) since the end of the Little Ice Age

R. Marti et al.

Title Page	
Abstract	Introduction
Conclusions	References
Tables	Figures
◀	▶
◀	▶
Back	Close
Full Screen / Esc	
Printer-friendly Version	
Interactive Discussion	



over polygons 1 to 4 (only these sectors were covered in 2006); and (ii) we calculated a mean geodetic mass balance assuming a density of 900 kg m^{-3} . We compared this geodetic mass balance to the corresponding glaciological mass balance. We obtained a difference of -0.68 m w.e. for $N = 5$ years, which gives $e_{\text{gla.total.a}} = +0.14 \text{ m w.e.}$

We estimated random errors due to the field measurements following the guidelines provided by Gerbaux et al. (2005). Given that only three occurrences of positive mass balance were observed over the whole period of record (88 measurements), the entire glacier was considered as an ablation zone over this period for the estimation of the errors (i.e we neglected the errors associated with the residual snow from the previous year). The mean annual error in the specific mass balance is $\sigma_{\text{glac.point.a}} = 0.15 \text{ m w.e.}$ The specific mean winter mass balance error is $\sigma_{\text{glac.point.w}} = 0.35 \text{ m w.e.}$ (Tab. 5).

Next, we estimated the random error due to the spatial integration $\sigma_{\text{glac.spatial.a}}$ to compute the glacier-wide glaciological mass balance from the specific mass balances. This was done using the DEMs made from the DGPS surveys performed in 2011 and 2012. For every polygon 1 to 6 (only these polygons were surveyed), we calculated the variance of the differences between both DEMs. The six variances values were aggregated based on Eq. (10), after rescaling the area weights. We obtained a mean value of 0.88 m w.e. However, this error value is likely too high, because, in part, it propagates the errors included in the DGPS DEMs. Therefore, we took $\sigma_{\text{glac.spatial.a}} = 0.7 \text{ m w.e.}$ We neglected the error term $\sigma_{\text{glac.ref.a}}$ due the changes in glacier area (Zemp et al., 2013). In sum, we estimated an annual total random error of $\sigma_{\text{glac.total.a}} = 0.85 \text{ m w.e.}$

The stake measurements performed from 1979 to 1985 followed similar protocol as that described above, except that the glacier was divided into 5 longitudinal sectors (Pont, 1985). We used the same annual total random error as for 2001–2013.

4.4 Glacier indicators combination

The Ossoue Glacier indicators mentioned above were pieced together to create a coherent time-line of glacier fluctuations. We defined five threshold values to classify variations in each glacier indicator over the period of record. We defined classes of

Evolution of Ossoue Glacier (French Pyrenees) since the end of the Little Ice Age

R. Marti et al.

Title Page

Abstract

Introduction

Conclusions

References

Tables

Figures

◀

▶

◀

▶

Back

Close

Full Screen / Esc

Printer-friendly Version

Interactive Discussion



markedly positive variations, positive variations, markedly negative variations, negative variations and a class of “no significant variation”. Classification in a positive or a negative class was based on whether the absolute annualized variation was equal or greater than the annualized random error (Tab. 6). If this condition was not fulfilled, the variation was classified as not significant for the period of record. From this classification, we qualitatively determined periods of stable-positive or negative evolution.

4.5 Geophysical surveys

A ground penetrating radar (GPR) survey was performed on 30–31 of August 2006 in the upper area of Ossoue Glacier. The GPR apparatus used was a PulseEkko 100 (Sensors and Software Inc.) with 50 MHz unshielded antennas. Three longitudinal profiles (W–E) running from the top to the slope transition of the glacier and four transverse profiles (N–S) were surveyed. The horizontal step was 0.5 m. The topography was acquired in real-time using a Leica DGNSS. In the radargrams strong reflectors identified at long two-way traveltimes were assumed to be the glacier bed. Hyperbolic features were used for electromagnetic (EM) velocity determination. An EM velocity of 0.16 m ns^{-1} was determined for the ice and was used to migrate the data. The thickness of the glacier was determined along the profiles at an horizontal resolution of 10 m. At the glacier margins the thickness was assumed to be zero (Saintenoy et al., 2013). The glacier thickness and surface elevation in 2006 were interpolated by ordinary kriging after second order trend removal (ESRI ArcGIS[®], Geostatistical Analyst tool). Subsequently a map of the subglacial bedrock elevation was generated. Based on the standard error map associated with kriging, we excluded the area in the prediction map where the kriging error was greater than $\sigma_{\text{krig}} = 10 \text{ m}$. From the 2013 glacier DEM and the bedrock map, we generated a 2013 glacier ice thickness map (Fig. 12). The mean random error for the subglacial elevation was calculated as follows:

$$\sigma_{\text{subglacial.total}} = \sqrt{\sigma_{\text{GPR}}^2 + \sigma_{\text{krig}}^2 + \sigma_{\text{bias.2006}}^2} \quad (14)$$

Evolution of Ossoue Glacier (French Pyrenees) since the end of the Little Ice Age

R. Marti et al.

Title Page

Abstract

Introduction

Conclusions

References

Tables

Figures

◀

▶

◀

▶

Back

Close

Full Screen / Esc

Printer-friendly Version

Interactive Discussion



Evolution of Ossoue Glacier (French Pyrenees) since the end of the Little Ice Age

R. Marti et al.

Title Page

Abstract

Introduction

Conclusions

References

Tables

Figures

◀

▶

◀

▶

Back

Close

Full Screen / Esc

Printer-friendly Version

Interactive Discussion

aged over summer periods (JJAS), winter periods (NDJFMA) and hydrological years (beginning 1 October). To reconcile the different recording periods of the meteorological and glaciological measurements, summer and annual mass balances were linearly interpolated by using a fixed date system (1 October, Cogley et al., 2011). The mass balances terms B_w were extrapolated to 31 May. Due to some missing data, it was not possible to calculate the mean annual temperature for several months at Gavarnie over the period 2002–2012. Thus we did not correlate these data with the annual mass balance.

We also used two monthly precipitation datasets:

- Monthly precipitation was recorded at the Gavarnie Valley station simultaneously with the temperature (see above for station location; period of record: January 1991 through May 2012).
- Monthly precipitation was recorded over the period 1882–2013 at Tarbes-Ossun Météo-France station (43.18° N 0.00° E, 360 m elevation, 50 km north-east of the glacier). These data were homogenized until 2000 and used as raw data since then (Moisselin et al., 2002).

Both datasets showed a significant correlation (Spearman's $\rho = 0.56$, p value < 0.01). We calculated annual and winter precipitations (NDJFMA). October and May precipitation values were not considered because the precipitation was as often liquid as solid in these months, and thus presumably does not contribute significantly to accumulation on the glacier. We performed correlations between precipitation and Ossoue Glacier winter and annual mass balance measurements over the 2001–2013 period considering a fixed date system (annual mass balances 1 October, winter mass balances 31 May). Due to some missing data, it was not possible to calculate the annual precipitation for several months at Gavarnie over the 2002–2012 period. Thus, we did not correlate these data with the annual mass balance.

We also considered the Atlantic Multidecadal Oscillation (AMO) and the North Atlantic Oscillation (NAO). Both indices represent fluctuations in the North Atlantic cli-

mate and have been successfully used in glacier-climate linkages (Six et al., 2001; Huss et al., 2010; Thibert et al., 2013).

- For the NAO we used a winter (DJFM) index based on the monthly 1850–1999 Climate Reasarch Unit (CRU) dataset, completed by Tim Osborn’s 2000–2013 NAO Update (Jones et al., 1997; Osborn, 2006). We applied a 5 yr moving average filter to smooth the signal.
- For the AMO we used the monthly index calculated from the Kaplan sea surface temperature dataset over 1861–2009 (Enfield et al., 2001).

5 Results

5.1 Front, outlines and area variations

Our reconstruction of the Ossoue Glacier front and area shows significant glacier retreat since the LIA, with intermittent stationary phases (Fig. 9).

From 1850 to 1889, the Ossoue Glacier front retreated by 346 m (-8.8 myr^{-1}). During the following fifteen years (1889–1904), the front position was quite stationary, retreating by 11 m between 1892 and 1893 and by only 9 m between 1899 and 1904. In the year 1904–1905, however the Ossoue Glacier front retreated by 23 m. The following periods were characterized by stability (1905–1911) and progression (1911–1927). In our dataset, the glacier reached its most position of greatest 20th century advance in 1927 (Tab. 7).

The area of Ossoue Glacier at the end of the LIA, based on moraines locations, was 112.6 ± 10 ha. The glacier area extracted from the “Etat Major” map (dated near 1851) is 115 ± 20 ha. Between the end of the LIA and 1924, the area of Ossoue Glacier decreased by 20 %. The area decreased by a further 10 % over the period 1924–1948. During the period 1948–1983 the front retreated by 315 m until 1963 and then advanced by 156 m, although the changes in area over this period were low (-3%). Over

Evolution of Ossoue Glacier (French Pyrenees) since the end of the Little Ice Age

R. Marti et al.

Title Page

Abstract

Introduction

Conclusions

References

Tables

Figures

◀

▶

◀

▶

Back

Close

Full Screen / Esc

Printer-friendly Version

Interactive Discussion



1983–2002 the area decreased by 17% with a notable width reduction on the slope transition. In the early 2000s, the area of Ossoue Glacier was less than 50% of the its area at the end of the LIA (Tab. 8).

Changes in glacier geometry mainly occurred in the lower part of the glacier. In the upper part, the glacier shape remained almost unchanged until 1983. From 1983 to 2013, glacier width reduced dramatically at the slope transition between the plateau and the tongue of the glacier.

5.2 Mass changes and ice thickness

Since 1924, Ossoue Glacier has lost a mean of 59 m.w.e. over the current glacier area (Fig. 9). The two periods of marked ice depletion, 1924–1948 and 1983–2013, were interrupted by a stable period between 1948 and 1983.

Between 1924 and 1948, the glacier lost -33.5 ± 8.8 m.w.e. (-1.39 m.w.e. yr^{-1}) over the 1948 glacier area and -25.5 ± 8.8 m.w.e. over the deglaciated margin. The ice depletion signal was strongest in the central part of the glacier (Fig. 7).

The period 1948–1983 is the only period with observed positive geodetic mass balance variation, with a cumulative value of $+5.8 \pm 2.6$ m.w.e. over the 1983 glacier area ($+0.16$ m.w.e. yr^{-1}). However, a notable depletion was observed on the tongue (Fig. 7). On the deglaciated margin, depletion was -7.9 ± 2.6 m.w.e. The glacier advanced over a very small area (1 ha) with a mean ice growth of 6.5 m.w.e. An area of higher accumulation is localized on the lower part of the glacier, below the slope transition (Fig. 7). At the end of that period, using ablation stakes, François Valla and Henri Pont measured mass gains of +0.81 m.w.e. in 1978, +0.26 m.w.e. in 1979, +0.17 m.w.e. in 1980, and 0 m.w.e. in 1981 and 1982. In 1983 and 1984, they considered the mass balances to be “negative” but did not provide quantitative information (Pont, 1985).

Over 1983–2013 the glacier lost -30.1 ± 1.7 m.w.e. over the 2013 glacier area (-1 m.w.e. yr^{-1}) and -22.6 ± 1.7 m.w.e. over the deglaciated margin. A marked pattern of ice depletion occurs along a longitudinal profile on the upper part of the glacier

Evolution of Ossoue Glacier (French Pyrenees) since the end of the Little Ice Age

R. Marti et al.

Title Page

Abstract

Introduction

Conclusions

References

Tables

Figures

◀

▶

◀

▶

Back

Close

Full Screen / Esc

Printer-friendly Version

Interactive Discussion

(Fig. 7). This phenomenon increases glacier convexity in that zone, which was once named as *Plateau des Neiges* in older maps.

If we consider the 2013 glacier area as a common integration area for all the periods, the absolute value of the geodetic mass balance increased over 1924–1948 (–35 m w.e.) and 1948–1983 (+6.1 m w.e.).

Between 2001 and 2013, superficial mass loss on Ossoue Glacier given by the glaciological method is 17.36 ± 2.9 m w.e. (-1.45 m w.e. yr⁻¹) (Fig. 8). The strongest mass losses were registered at the lowest elevated stakes (stakes 7 and 8). The mass balance was negative every year since the stake measurements began except in 2012–2013 with a value of +0.22 m w.e. (René et al., 2014). In 2008 the mass balance was only slightly negative.

In 2006, the estimated mean ice thickness was 29.3 ± 6.3 m (max. 74.8 ± 10.2 m), giving an estimate of 25 ± 6.5 m (max. 59 ± 10.3 m) in 2013 (Fig. 12). In 2011, another GRP survey (Del Rio et al., 2012) indicated a maximum depth of 45 m and an average depth of 30 m. Despite the discrepancies in ice thickness, both studies suggest similar bedrock morphologies. As a verification of these data, we provide here the depth of the main moulins that have been measured regularly since 2004 by glacial speleologists: 30 m in 2004, 38 m in 2005, 36.5 m in 2006 and 41.5 m in 2009. However, these values should be considered minimum estimates of the glacier thickness because they do not necessarily reach the bedrock.

5.3 Trends observed from glacier indicators

Taken together, all indicators suggest a clear retreat of Ossoue Glacier since the end of the LIA (Fig. 10). We identified three periods of marked ice depletion, when these indicators consistently indicate a negative trend: 1850–1890, 1928–1950 and 1983–2013. By the same reasoning, two periods are characterized by stability or slightly growth: 1905–1928 and 1950–1983.

Evolution of Ossoue Glacier (French Pyrenees) since the end of the Little Ice Age

R. Marti et al.

Title Page

Abstract

Introduction

Conclusions

References

Tables

Figures

◀

▶

◀

▶

Back

Close

Full Screen / Esc

Printer-friendly Version

Interactive Discussion



5.4 Linkage with climate

Correlations between the Ossoue Glacier mass balances time series (2001–2013) indicate that the annual mass balance is mainly dependent on the summer mass balance and that the winter mass balance has less influence (Spearman's $\rho = 0.84$ for summer mass balance and $\rho = 0.65$ for winter mass balance).

The link between ablation and air temperature is verified at Ossoue Glacier through the high and significant (p value < 0.05) correlations between monthly summer ablation and monthly air temperature time series over 2002–2013 ($\rho = -0.81$ for Gavarnie valley station, $\rho = -0.74$ for Pic du Midi station, which is located farther from the glacier, and $\rho = -0.8$ for the regional CRU time series). Mean summer air temperature and summer-wide mass balance B_s (June–September) are also correlated, although only significantly with the Gavarnie dataset ($\rho = -0.72$ for Gavarnie, $\rho = -0.52$ for Pic du Midi and $\rho = -0.66$ for the CRU time series). The high correlation between the different time series over the common period of records ($\rho > 0.96$, p values < 0.05) give us confidence that the mean summer temperature at Pic du Midi is related to B_s .

The link between annual mass balance and mean annual temperature is weaker in the Pic du Midi time series than in the CRU time series ($\rho = -0.45$ for Pic du Midi and $\rho = -0.74$ for the CRU time series). The correlation is only significant with the CRU dataset. This may due to the use of raw data in the Pic du Midi time series starting from 2011 or to the limited period of record of glaciological mass balance (annual mass balance measurements only began in 2001). However, due to the good correlation between the CRU and the Pic du Midi temperature datasets, we also considered that the mean annual temperature at Pic du Midi is linked to $B_{\text{glac.a}}$ over the longer period 1890–2013. The elevation of the Pic du Midi station (2874 m a.s.l.) is close to that of the Ossoue Glacier front (2755 m a.s.l.); thus, we used principally this dataset to identify temperature trends over historical periods.

Precipitations records at Gavarnie and Tarbes are significantly correlated with the winter mass balances ($\rho = 0.71$ for Gavarnie, $\rho = 0.69$ for Tarbes, which is located far-

TCD

9, 2431–2494, 2015

Evolution of Ossoue Glacier (French Pyrenees) since the end of the Little Ice Age

R. Marti et al.

Title Page

Abstract

Introduction

Conclusions

References

Tables

Figures

◀

▶

◀

▶

Back

Close

Full Screen / Esc

Printer-friendly Version

Interactive Discussion



ther from the glacier). The link between annual mass balance and annual precipitation is significant in the Tarbes dataset ($\rho = 0.66$). Thus, we conclude that the Tarbes time series can be used to identify trends in precipitation that are linked with Ossoue Glacier fluctuations.

5 The mean annual temperature over the hydrological year (starting 1 October) and the mean summer temperature (JJAS) over 1858–2013 are -1.1 and 5.1 °C, respectively. The annual precipitation and the winter precipitation (NDJFMA) over 1882–2013 are 1068.2 and 556 mm, respectively. Analysis of temperature and precipitation trends over the six periods from a combination of indicators (Fig. 10) reveals four significant trends:

- 10 – The mean annual temperature over 1858–1890 may have continuously decreased. Over the same period, the mean summer temperature (JJAS) is slightly higher than the mean summer temperature over 1858–2013 (5.3 °C).
- The annual precipitation trend over 1950–1982 is positive ($\rho = 0.42$) and equal to the mean precipitation over 1882–2013 (1068 mm). Winter precipitation is higher than the mean recorded over 1882–2013 (586.2 mm). The annual mean temperature (-1.4 °C) and mean summer temperature (4.8 °C) are lower than the means over 1858–2013.
- 15 – The last period considered (1983–2013) shows positive trends in both mean annual and mean summer temperature, with the highest registered mean temperatures (-0.4 °C for annual and 6.1 °C for summer).

6 Discussion

Using multiple datasets, we generated five independent time series of glacier indicators (length, area, thickness at Villa Russell, geodetic and glaciological mass balances variations) to reconstruct the evolution of Ossoue Glacier since the end of the LIA (Fig. 10).

25 The indicators give a generally consistent chronology of glacier fluctuations since the

TCO

9, 2431–2494, 2015

Evolution of Ossoue Glacier (French Pyrenees) since the end of the Little Ice Age

R. Marti et al.

Title Page

Abstract

Introduction

Conclusions

References

Tables

Figures

◀

▶

◀

▶

Back

Close

Full Screen / Esc

Printer-friendly Version

Interactive Discussion



Evolution of Ossoue Glacier (French Pyrenees) since the end of the Little Ice Age

R. Marti et al.

Title Page

Abstract

Introduction

Conclusions

References

Tables

Figures

◀

▶

◀

▶

Back

Close

Full Screen / Esc

Printer-friendly Version

Interactive Discussion

LIA, although there are some discrepancies. We should bear in mind that the indicators do not directly reflect the same glaciological processes. The time series of frontal variations offers the best temporal resolution to of the onset of glacier changes, but these changes are strongly influenced by ice dynamics. Glacier motion is dependent on mass variations on the upper part of the glacier, but the response time is largely unknown. Areal variations depend on ice thickness at the edges only. Thickness variations registered at Villa Russell are the result of accumulation and ablation variations at the northern periphery of the glacier only, which could be prone to snow drifting. Volumetric mass changes generated by the geodetic method are mostly the result of the surface energy budget but also include internal and basal mass variations, which remain difficult to estimate. Glaciological mass balance reflects the link between energy and mass budget well, but can only be measured at a limited sample of points of the glacier surface. However, these indicators are all sensitive to the glacier mass changes, with different times scales and intensities of response. For instance, between 1948 and 1983, the mass balance was positive, but frontal variations were negative until 1963. This can likely be explained by the delay in the response time of frontal response to glacier mass changes. In the case of Ossoue Glacier, it is note-worthy that the indicators over the study period reveal a consistent signal (Fig. 10).

The evolution of Ossoue Glacier is consistent with the reconstructed evolutions of other Pyrenean glaciers. It is in good agreement with Cía et al. (2005) (Maladeta Glacier, 42.65° N, 0.64° E, northeast-oriented, 2870–3200 m altitude range and 0.27 km² area in 2011) and with Chueca et al. (2003) (Coronas Glacier, a glacieret or ice patch since the 2000s, 42.63° N, 0.65° E, southwest-oriented, 3100–3240 m and 0.02 km² in 2011) and Gellatly et al. (1994) (Taillon Glacier, 42.69° N, -0.04° E, northeast-oriented, 2530–2800 m, 0.08 km² in 2011). Considering an accuracy of ±5 years, two common stable periods could be identified (1905–1930 and 1955–1985) as well as two periods of marked ice depletion (1850–1900 and from mid-1980s until now). The evidence of strong marked ice depletion found in this study for Ossoue Glacier between 1924 and 1948 ($-1.39 \text{ m m.w.eyr}^{-1}$) should be considered with cau-

Evolution of Ossoue Glacier (French Pyrenees) since the end of the Little Ice Age

R. Marti et al.

Title Page

Abstract

Introduction

Conclusions

References

Tables

Figures

◀

▶

◀

▶

Back

Close

Full Screen / Esc

Printer-friendly Version

Interactive Discussion

tion given the high uncertainties in the altimetry restitution process. However, reconstructions of other Pyrenean glaciers over comparable periods tend to corroborate this result. Between approximately 1928 and 1957, the length of Coronas Glacier decreased from 600 to 350 m, while its area decreased from 19 to 8.6 ha and its equilibrium line altitude (ELA) increased from 3065 to 3122 m (Chueca Cía et al., 2001). During the period 1935–1957, Maladeta Glacier lost 15 ha (-0.68 ha yr^{-1}) and its length decreased by 80 m. This retreat is assumed to be due to a warm anomaly detected in the second half of the 1940s (Cía et al., 2005). The Maladeta Glacier mass balance time series (1991–2013) shows a good agreement with Ossoue glaciological mass balances time series over the period 2001–2013 (Fig. 9). During the 1990s, the Maladeta mass balance values were slightly negative. If we compare the Ossoue geodetic mass balance during 1983–2013 ($-1 \text{ m w.e. yr}^{-1}$) and the Ossoue glaciological mass balance during 2001–2013 ($-1.45 \text{ m w.e. yr}^{-1}$), we can deduce that the 1983–2001 Ossoue ablation rate was approximately $-0.7 \text{ m w.e. yr}^{-1}$. This result is consistent with the aforementioned variations of the Maladeta Glacier over 1991–2001 (Fig. 9).

In the French Alps, which is the nearest glaciated massif to the Pyrenees, two steady-state periods (1907–1941 and 1954–1981) and two periods of recession (1942–1953 and 1982–1999) were deduced from four glacier mass balances time series (Vincent, 2002). This further suggests that there is a common climatic driver governing fluctuations in Pyrenean and Alpine glaciers since the LIA.

Figure 11 provides insight into the possible linkage between the evolution of the Ossoue Glacier and the regional-scale climate. The period 1960–1980 is characterized by a succession of negative phases of the NAO, this coincides with a period of relative glacier growth or stability (positive variations in various glacier lengths, areas and mass balances). Ossoue Glacier seems to be anti-correlated with the NAO. Similar results were reported by Six et al. (2002) and Marzeion et al. (2014) for glaciers of the southern Alps. In addition, variations in the AMO index also appear relatively similar to variations in the combined Ossoue Glacier indicators throughout the 20th century. This result is consistent with previous studies on the influence of the multidecadal internal variability

of the North Atlantic circulation on the Northern Hemisphere climate (e.g., Enfield et al., 2001).

Variations of Ossoue Glacier indicators are in good agreements with meteorological data: periods of ice depletion are generally characterized by lower values of mean precipitation and temperatures (Tab. 13). The evolution of Ossoue Glacier may be partially explained by observed trends, with a significant positive trend in 1950–1982 precipitations (a stable period for the glacier) and a significant constant rise in mean annual and summer temperature since 1983 (a period of depletion for the glacier). The periods 1850–1890 and 1983–2013 are marked by ice depletion, although the mean air temperature time series have opposite and significant trends. Frontal variations and mean air temperature variations over the 1850–1890 interval point to a shorter period of marked ice depletion, 1850–1874, with lesser depletion over the 1874–1890 period. By the same reasoning the selected 1928–1950 period of ice depletion period may have been more pronounced in the 1937–1950 “subperiod” than over the 1928–1937 “subperiod”.

The future evolution of Ossoue Glacier depends on climatic changes, but is also constrained by the remaining ice volume. Considering the remaining ice depth in 2013 and assuming that the Ossoue Glacier mass balance follows the same trend as that recorded during 2001–2013 ($-1.45 \text{ m.w.e. yr}^{-1}$), the glacier should totally disappear in 40 years. To further illustrate this, the ice thickness map (Fig. 12) was divided with thickness classes that are multiples of 1.5, i.e., a value close to the current annual mass loss rate. Thus, this map gives a rough estimation of the evolution of the glacier area every eight years. Based on this map and the past evolution of the glacier, we anticipate that the glacier may split into two parts at the slope transition (Fig. 4) in the near future. At this location the glacier may be particularly thin, and there is an abrupt change in the glacier slope. The lowest part may soon no longer be fed by the ice flow from the upper area and could thus rapidly disappear. This separation would drastically change the morphology of Ossoue Glacier from an active glacier to a glacieret or ice

Evolution of Ossoue Glacier (French Pyrenees) since the end of the Little Ice Age

R. Marti et al.

Title Page

Abstract

Introduction

Conclusions

References

Tables

Figures

◀

▶

◀

▶

Back

Close

Full Screen / Esc

Printer-friendly Version

Interactive Discussion



patch. Such glacier fragmentation has been regularly observed on Pyrenean glaciers, e.g., the neighboring Petit Vignemale and Oulettes Glaciers.

However, future evolution of Ossoue Glacier based on interpretation of Fig. 12 was made under several strong assumptions: (i) the mass balance patterns are uniform, (ii) ice motion can be neglected, and (iii) the mass loss in the future decades will occur at the same pace as during the last decade. Our data suggest that the uniform mass balance assumption is questionable. Geodetic measurements over 1983–2013 show a clear depression in the central part of the glacier, which indicates that the glacier evolves toward a more convex topography. Stake measurements over 2001–2013 reflect the influence of the glacier topography, principally in the ablation period (Tab. 4 and Fig. 8). Accumulation processes do not show a vertical gradient, but may show a north–south gradient in the upper part, most likely driven by the accumulation of wind-blown snow. Elevation is the main factor that separates the three groups of stakes: above the glaciological mass balance (stakes 1 to 3), slightly beneath (stakes 3 and 5) and beneath (stakes 7 and 8). Stake 6 shows uncommon behavior that is most likely influenced by greater ice motion at that location. The influence of the aspect explains the discrepancy between stake 2 and stake 4, while slope seems to explain the higher melting rate at stake 3 compared to the lower-elevation stake 5. Future work is necessary to better understand the effect of local topography on the spatial variability of glacier mass balance. This influence is expected to augment in the future as the glacier retreats (López-Moreno et al., 2006a, b).

If the current ablation rate continues, Ossoue Glacier will disappear halfway through the 21st century. Its large, markedly convex plateau (two thirds of the present-day area) has allowed the accumulation of a significant amount of ice at high altitude (3105 m) during favorable periods. However, due to the limited interval range of the plateau (3030–3200 m, slope 8°), any future rise of the lower limit of the glacier (2755 m in 2013) would drastically modify the responses of the indicators of Ossoue Glacier to future climate fluctuations.

Evolution of Ossoue Glacier (French Pyrenees) since the end of the Little Ice Age

R. Marti et al.

Title Page

Abstract

Introduction

Conclusions

References

Tables

Figures

◀

▶

◀

▶

Back

Close

Full Screen / Esc

Printer-friendly Version

Interactive Discussion



7 Conclusions

Ossoue Glacier is one of the southernmost glaciers in Europe. Using an exceptional archive of historical datasets and recent accurate observations, we generate consistent time series of various glacier indicators such as length, area, elevation variations, and mass changes since the LIA at high temporal resolution. The dominant trend is a retreat over the 20th century, which was interrupted by two stable periods, 1906–1924 and 1960–1983. These periods appear to be roughly in phase with hemispheric climate proxies such as the North Atlantic Oscillation and the Atlantic Multidecadal Oscillation. The 1960–1980 stable period may be partially explained by anti-correlation to the NAO index. We found that the ablation rate may have doubled in the last decade, likely as a result of the recent climate warming.

The evolution of Ossoue Glacier is in good agreement with that of other Pyrenean glacier reconstructions (Maladeta, Coronas, Taillon Glaciers) suggesting the possibility of long-term high-elevation climate reconstruction in the Pyrenees.

The time resolution of the generated indicators allows us to extract consistent glacier changes over various periods. These generally concur with climatic data, suggesting that Ossoue Glacier is a good regional climate proxy. However, it remains difficult to isolate the relative contribution of precipitation and air temperature changes to the reconstructed mass balance variations. This could be achieved with a temperature index model or a more sophisticated glacier model (e.g., Gerbaux et al., 2005).

The eastern orientation and low shading of Ossoue Glacier make it particularly vulnerable to climate fluctuations, although its relatively high elevation supports large amounts of snow accumulation. Windblown snow could also increase accumulation on some parts of the glacier.

Future studies should focus on topo-climatic drivers of Ossoue Glacier mass balance in an effort to better understand the link between its past temporal evolution and regional climate change.

Evolution of Ossoue Glacier (French Pyrenees) since the end of the Little Ice Age

R. Marti et al.

Title Page

Abstract

Introduction

Conclusions

References

Tables

Figures



Back

Close

Full Screen / Esc

Printer-friendly Version

Interactive Discussion



More generally, retreat of Pyrenean glaciers could affect local ecosystems by diminishing the beta diversity in Pyrenean streams (Finn et al., 2013). Natural patrimony and the visual perception of the high mountain landscape could also be irrevocably affected (EDYTEM, 2009; Moreau, 2010; René, 2013).

5 *Acknowledgements.* The authors warmly thank all the volunteers who provided great help during fieldwork, especially the members of the Association Moraine. This work was supported by the *Fondation Eau, Neige et Glace* (www.fondation-eng.org) and the *Region Midi-Pyrénées* through the CRYOPYR and CLIM Ex-PYR projects. We also thank Patrick Wagnon, who kindly sponsored the CLIM Ex-PYR project.

10 References

Boé, J. and Habets, F.: Multi-decadal river flow variations in France, *Hydrol. Earth Syst. Sci.*, 18, 691–708, doi:10.5194/hess-18-691-2014, 2014. 2437

Bonaparte, p. R.: Les variations périodiques des glaciers français, *Typographie Chamerot et Renouard*, available at: <http://www.worldcat.org/title/variations-periodiques-des-glaciers-francais/oclc/6549420> (last access: 8 April 2015), 1892. 2436

Bücher, A. and Dessens, J.: Secular trend of surface temperature at an elevated observatory in the Pyrenees, *J. Climate*, 4, 859–868, doi:10.1175/1520-0442(1991)004<0859:STOSTA>2.0.CO;2, 1991. 2434, 2449

20 Büntgen, U., Frank, D., Grudd, H. K., and Esper, J.: Long-term summer temperature variations in the Pyrenees, *Clim. Dynam.*, 31, 615–631, doi:10.1007/s00382-008-0390-x, 2008. 2434

Camberlin, P. and Yves, R. (Eds.): XXVII AIC (International Climate association) Symposium, vol. I, AIC (Association Internationale de Climatologie), Dijon, France, 2–5 July 2014, 344–350, available at: http://www.aic2014.com/congressr/document/Actes_AIC_2014.pdf (last access: 8 April 2015), 2014. 2434

25 Cazenave-Piarrot, F., Egels, Y., and Tihay, J.: L'évolution récente du glacier d'Ossoue (Pyrénées centrales), GEGP. IGN, Université de Pau et des Pays de l'Adour, Pau, France, 1987. 2436, 2440

Evolution of Ossoue Glacier (French Pyrenees) since the end of the Little Ice Age

R. Marti et al.

Title Page

Abstract

Introduction

Conclusions

References

Tables

Figures

◀

▶

◀

▶

Back

Close

Full Screen / Esc

Printer-friendly Version

Interactive Discussion



Evolution of Ossoue Glacier (French Pyrenees) since the end of the Little Ice Age

R. Marti et al.

Title Page

Abstract

Introduction

Conclusions

References

Tables

Figures

◀

▶

◀

▶

Back

Close

Full Screen / Esc

Printer-friendly Version

Interactive Discussion

- Chueca, J. and Julian, A.: Relationship between solar radiation and the development and morphology of small cirque glaciers (Maladeta Mountain massif, Central Pyrenees, Spain), *Geogr. Ann. A*, 86, 81–89, doi:10.1111/j.0435-3676.2004.00215.x, 2004. 2437
- Chueca, J., Julián, A., and López, I.: Variations of Glaciar Coronas, Pyrenees, Spain, during the 20th century, *J. Glaciol.*, 49, 449–455, doi:10.3189/172756503781830674, 2003. 2437, 2456
- Chueca, J., Julian, A., and René, P.: Estado de los glaciares en la cordillera pirenaica (vertientes española y francesa) a finales del siglo XX, in: *Contribuciones recientes sobre geomorfología*, edited by: Benito, G. and Díez Herrero, A., *Actas VIII Reunión Nacional de Geomorfología*, SEG-CSIC, 91–102, Madrid, Spain, 2004. 2435
- Chueca, J., Julián, A., and López-Moreno, J. I.: Recent evolution (1981–2005) of the Maladeta glaciers, Pyrenees, Spain: extent and volume losses and their relation with climatic and topographic factors, *J. Glaciol.*, 53, 547–557, doi:10.3189/002214307784409342, 2007. 2434, 2435, 2437, 2438
- Chueca, J., Julian, A., and Lopez, I.: The Retreat of the Pyrenean Glaciers (Spain) from the Little Ice Age: Data Consistency and Spatial Differences, *Terra Glacialis*, 11, 65–77, Special issue, January 2009, Servizio Glaciologico Lombardo, Italy, 2008. 2437, 2438
- Chueca Cía, J., Julian Andres, A., Saz Sanchez, M., Creus Novau, J., Lopez-Moreno, I., and Lapena Laiglesia, A.: Estudio de la evolución del glaciar de Coronas (Macizo de la Maladeta; Pirineo Central español) desde el final de la pequeña edad del hielo hasta la actualidad, y de su relación con el clima, *Boletín glaciológico aragonés*, ISSN 1695-7989, 2, 81–115, available at: <http://dialnet.unirioja.es/servlet/articulo?codigo=1975440> (last access: 8 April 2015), 2001. 2457
- Cía, J. C., Andrés, A. J., Sánchez, M. S., Novau, J. C., and Moreno, J. L.: Responses to climatic changes since the Little Ice Age on Maladeta Glacier (Central Pyrenees), *Geomorphology*, 68, 167–182, doi:10.1016/j.geomorph.2004.11.012, 2005. 2437, 2456, 2457
- Cogley, J. G., Hock, R., Rasmussen, L. A., Arendt, A. A., Bauder, A., Jansson, P., Braithwaite, R. J., Kaser, G., Möller, M., Nicholson, L., Zemp, M.: Glossary of Glacier Mass Balance and Related Terms, Paris, UNESCO-IHP (IHP-VII Technical documents in hydrology, 86, IACS contribution 2), 2011. 2438, 2444, 2445, 2446, 2450, 2480, 2481
- Courraud, L.: Reconstitution des données de températures mensuelles manquantes du Pic du Midi de Bigorre, Rapport de stage: INP Toulouse/ENM, Institut National Polytechnique de Toulouse, Toulouse, France, 2011. 2449

Evolution of Ossoue Glacier (French Pyrenees) since the end of the Little Ice Age

R. Marti et al.

Title Page

Abstract

Introduction

Conclusions

References

Tables

Figures

◀

▶

◀

▶

Back

Close

Full Screen / Esc

Printer-friendly Version

Interactive Discussion

tandfonline.com/doi/abs/10.1080/02723646.1994.106425253.VSU7V5MhFSA (last access: 8 April 2015), 1994. 2436, 2437, 2456

Gerbaux, M., Genthon, C., Etchevers, P., Vincent, C., and Dedieu, J. P.: Surface mass balance of glaciers in the French Alps: distributed modeling and sensitivity to climate change, *J. Glaciol.*, 51, 561–572, doi:10.3189/172756505781829133, 2005. 2445, 2447, 2460, 2474

Giuntoli, I., Renard, B., Vidal, J.-P., and Bard, A.: Low flows in France and their relationship to large-scale climate indices, *J. Hydrol.*, 482, 105–118, doi:10.1016/j.jhydrol.2012.12.038, 2013. 2437

GLACIOCLIM: Service d'Observation: GLACIOCLIM, available at: <http://www-igge.obs.ujf-grenoble.fr/ServiceObs/> (last access date: 8 April 2015), 2001. 2445

Grove, J. M.: *Little Ice Ages: Ancient and Modern*, Taylor & Francis, ISBN0415334233, 9780415334235, 2004. 2435, 2439

Grunewald, K. and Scheithauer, J.: Europe's southernmost glaciers: response and adaptation to climate change, *J. Glaciol.*, 56, 129–142, doi:10.3189/002214310791190947, 2010. 2434, 2437

Guilhot, N.: *Histoire d'une parenthèse cartographique: les Alpes du Nord dans la cartographie topographique française aux 19e et 20e siècles*, Lyon 2, available at: <http://www.theses.fr/2005LYO20047> (last access: 8 April 2015), 2005. 2440

Hoelzle, M., Chinn, T., Stumm, D., Paul, F., Zemp, M., and Haeberli, W.: The application of glacier inventory data for estimating past climate change effects on mountain glaciers: a comparison between the European Alps and the Southern Alps of New Zealand, *Global Planet. Change*, 56, 69–82, doi:10.1016/j.gloplacha.2006.07.001, 2007. 2437

Hoffman, M. J., Fountain, A. G., and Achuff, J. M.: 20th-century variations in area of cirque glaciers and glacierets, Rocky Mountain National Park, Rocky Mountains, Colorado, USA, *Ann. Glaciol.*, 46, 349–354, doi:10.3189/172756407782871233, 2007. 2441

Huss, M.: Density assumptions for converting geodetic glacier volume change to mass change, *The Cryosphere*, 7, 877–887, doi:10.5194/tc-7-877-2013, 2013. 2443

Huss, M., Hock, R., Bauder, A., and Funk, M.: 100-year mass changes in the Swiss Alps linked to the Atlantic Multidecadal Oscillation, *Geophys. Res. Lett.*, 37, L10501, doi:10.1029/2010GL042616, 2010. 2451

Hutchinson, M. F.: *ANUDEM version 5.3, user guide*, Fenner School of Environment and Society, Australian National University, Canberra, available at: http://fennerschool.anu.edu.au/files/usedem53_pdf_16552.pdf (last access: 8 April 2015), 2011. 2441

Evolution of Ossoue Glacier (French Pyrenees) since the end of the Little Ice Age

R. Marti et al.

[Title Page](#)[Abstract](#)[Introduction](#)[Conclusions](#)[References](#)[Tables](#)[Figures](#)[◀](#)[▶](#)[◀](#)[▶](#)[Back](#)[Close](#)[Full Screen / Esc](#)[Printer-friendly Version](#)[Interactive Discussion](#)

temperature and precipitation winter modes in the Mediterranean mountains: observed relationships and projections for the 21st century, *Global Planet. Change*, 77, 62–76, doi:10.1016/j.gloplacha.2011.03.003, 2011. 2437

Marti, R., Gascoïn, S., Houet, T., and Laffly, D.: Assessment of a glacier digital elevation model generated from Pléiades stereoscopic images: Ossoue Glacier, Pyrenees, France, in: *Pléiades Days 2014*, Toulouse, France, 1 April 2014, http://espace-ftp.cborg.info/pleiades_days/presentations2014/GO2_Marti.pdf (last access: 8 April 2015), 2014. 2442

Marzeion, B., Cogley, J. G., Richter, K., and Parkes, D.: Attribution of global glacier mass loss to anthropogenic and natural causes, *Science*, 345, 919–921, 1254702, doi:10.1126/science.1254702, 2014. 2457

Meillon, A. and de Larminat, E.: Notice sur la carte au vingt millième 20000e avec l'explication des noms de lieux et de montagnes de la région de Cauterets, Marrimpouey, Pau, France, 1933. 2440

Mercanton, P. L.: Commission on snow and ice, reports from 1936 to 1956, *International Association of Scientific Hydrology, IAHS*, 30 (1948), 233–261 (Paris), *IAHS*, 32 (1952), 107–119 (Paris), *IAHS*, 39 (1954), 478–490 (Paris), *IAHS*, 46 (1958), 358–371 (Paris), 1956. 2436

Moisselin, J.-M., Schneider, M., and Canellas, C.: Les changements climatiques en France au XX^e siècle. Etude des longues séries homogénéisées de données de température et de précipitations, available at: <http://documents.irevues.inist.fr/handle/2042/36233> (last access: 8 April 2015), 2002. 2450

Moreau, M.: Visual perception of changes in a high mountain landscape: the case of the retreat of the Évettes Glacier (Haute-Maurienne, northern French Alps), *Géomorphologie: relief, processus, environnement*, 2, 165–174, doi:10.4000/geomorphologie.7901, 2010. 2461

Osborn, T. J.: Recent variations in the winter North Atlantic Oscillation, *Weather*, 61, 353–355, doi:10.1256/wea.190.06, 2006. 2451

Ostrem-Brugman: Glacier Mass-Balance Measurements: a Manual for Field and Office Work, NHRI Science Report, Geographisches Institut Universität, Zürich, 224 pp., 1991. 2445

Pont, H.: Contribution à l'Etude des Glaciers du Taillon et d'Ossoue, Tech. rep., Parc National des Pyrénées, Tarbes, France, 1985. 2436, 2447, 2452

Pont, H. and Valla, F.: Observations glaciologiques dans les Pyrénées, Tech. rep., Société Hydrotechnique de France, Paris, France, 1980. 2436

Racoviteanu, A. E., Paul, F., Raup, B., Khalsa, S. J. S., and Armstrong, R.: Challenges and recommendations in mapping of glacier parameters from space: re-

Evolution of Ossoue Glacier (French Pyrenees) since the end of the Little Ice Age

R. Marti et al.

Title Page

Abstract

Introduction

Conclusions

References

Tables

Figures

◀

▶

◀

▶

Back

Close

Full Screen / Esc

Printer-friendly Version

Interactive Discussion

sults of the 2008 Global Land Ice Measurements from Space (GLIMS) workshop, Boulder, Colorado, USA, Ann. Glaciol., 50, 53–69, available at: <http://www.ingentaconnect.com/content/igsoc/agl/2010/00000050/00000053/art00008>

[http://www.researchgate.net/publication/228649051_Challenges_and_recommendations_in_mapping_of_glacier_parameters_from_space_results_of_the_2008_Global_Land_Ice_Measurements_from_Space_\(GLIMS\)_workshop_/file/d912f50b4b6e5ef2c9.pdf](http://www.researchgate.net/publication/228649051_Challenges_and_recommendations_in_mapping_of_glacier_parameters_from_space_results_of_the_2008_Global_Land_Ice_Measurements_from_Space_(GLIMS)_workshop_/file/d912f50b4b6e5ef2c9.pdf) (last access: 8 April 2015), 2010. 2442

Radok, U.: The International Commission on Snow and Ice (ICSI) and its precursors, 1894–1994, Hydrolog. Sci. J., 42, 131–140, doi:10.1080/02626669709492015, 1997. 2436

Reid, H. and Muret, E.: Les variations périodiques des glaciers, XI^{me} Rapport, Zeitschrift für Gletscherkunde und Glazialgeologie I, 1–21, Archives des Sciences physiques et naturelles, 110/4 (20), Genève, Switzerland, 1905, 1906. 2483

René, P.: Glaciers des Pyrénées, Editions CAIRN, available at: <http://geomorphologie.fr/glaciers-des-pyrenees-pierre-rene/> (last access: 8 April 2015), 2013. 2445, 2461

René, P.: Monitoring of glaciers in the French Pyrenees, available at: <http://hdl.handle.net/2042/53748> <http://documents.irevues.inist.fr/handle/2042/53748> (last access date: 8 April 2015), 2014. 2435, 2436

René, P., Marti, R., Gascoin, S., Houet, T., and Laffly, D.: Le glacier d'Ossoue (Pyrénées françaises): 2013, premier bilan de masse positif de la série, in: Journées SHF Glaciologie – Nivologie – Hydrologie de Montagne, Grenoble, 20 and 21 March 2014, p. 2, http://www.shf-hydro.org/174-1-journees_glaciologie_nivologie_hydrologie_de_montagne-16.html (last access: 8 April 2015), 2014. 2453

Saintenoy, A., Friedt, J.-M., Booth, A. D., Tolle, F., Bernard, E., Laffly, D., Marlin, C., and Griselin, M.: Deriving ice thickness, glacier volume and bedrock morphology of the Austre Lovenbreen (Svalbard) using Ground-penetrating Radar, arXiv preprint, arXiv:1306.2539, available at: <http://arxiv.org/abs/1306.2539> (last access: 8 April 2015), 2013. 2448

Schrader, F.: Sur l'étendue des glaciers des Pyrénées (On the extent of the glaciers of the Pyrenees): Paris, Annuaire de Club Alpin Français, v. 21, edition Privat-Didier Toulouse 1936, Paris, France, 1895. 2435

Serrat, D. and Ventura J.: US Geological Survey Professional Paper 1386-E-2 Satellite Image Atlas of Glaciers of the World E-2, Glaciers of the Pyrenees, Spain and France, edited by: Williams, Jr., R. S. and Ferrigno, J. G., available at: <http://pubs.usgs.gov/pp/p1386e/> (last access date: 8 April 2015), US Geological Survey Professional Paper 1386-E, 1988. 2435

observations_a_review_of_the_worldwide_monitoring_network/file/504635253d1e0cc608.pdf (last access date: 8 April 2015), 2009. 2434

5 Zemp, M., Thibert, E., Huss, M., Stumm, D., Rolstad Denby, C., Nuth, C., Nussbaumer, S. U., Moholdt, G., Mercer, A., Mayer, C., Joerg, P. C., Jansson, P., Hynek, B., Fischer, A., Escher-Vetter, H., Elvehøy, H., and Andreassen, L. M.: Reanalysing glacier mass balance measurement series, *The Cryosphere*, 7, 1227–1245, doi:10.5194/tc-7-1227-2013, 2013. 2442, 2444, 2446, 2447

TC D

9, 2431–2494, 2015

Evolution of Ossoue Glacier (French Pyrenees) since the end of the Little Ice Age

R. Marti et al.

Title Page

Abstract

Introduction

Conclusions

References

Tables

Figures

◀

▶

◀

▶

Back

Close

Full Screen / Esc

Printer-friendly Version

Interactive Discussion



Evolution of Ossoue Glacier (French Pyrenees) since the end of the Little Ice Age

R. Marti et al.

Table 3. Meta-data of Ossoue Glacier volumetric measurements errors. Mean elevation bias ϵ_{bias} and SD σ_{bias} are based on DGPS points surveyed on the deglaciated margin. The symbol * means that the bias was removed from the final DEM (Sect. 4.2) and was not taken into account in the total error. ϵ_t refers to the systematic error due to the timelag between the survey date and 1 October (Sect. 4.2). The term σ_{dc} refers to the density conversion error. The last columns are the sums of systematic and random errors for the period of record (PoR). The propagation law is applied for random errors (root sum of squares).

Derived 2 m-DEM $t_1 - t_2$	DEM t_1 (ϵ_{bias} ; σ_{bias})	DEM t_2 (ϵ_{bias} ; σ_{bias})	Errors on DEMs Differences (in m.w.e.)				
			ϵ_{t_1}	ϵ_{t_2}	σ_{dc}	$\epsilon_{\text{total.PoR}}$	$\sigma_{\text{total.PoR}}$
1924–1948	($\epsilon_{\text{bias.1924}}$; 8.6)	(-1.8*; 2)	+1.71	+0.94	–	2.65 + $\epsilon_{\text{bias.1924}}$	8.8
1948–1983	(-1.8*; 2)	(-1.4*; 1.6)	+0.94	+1.41	0.32	2.35	2.6
1983–2013 Pléiades	(-1.4*; 1.6)	(-1.37*; 1.8)	+1.41	+0.42	–	1.83	2.4
1983–2013 DGPS	(-1.4*; 1.6)	(0; 0.6)	+1.41	0	–	1.41	1.7

Title Page

Abstract

Introduction

Conclusions

References

Tables

Figures

◀

▶

◀

▶

Back

Close

Full Screen / Esc

Printer-friendly Version

Interactive Discussion

Evolution of Ossoue Glacier (French Pyrenees) since the end of the Little Ice Age

R. Marti et al.

Table 4. Topographic characteristics (2013) by glaciological sectors (polygons) S_k , where k is the stake number.

	S_1	S_2	S_3	S_4	S_5	S_6	S_7	S_8
Mean elevation	3151 m	3115 m	3093 m	3100 m	3060 m	2981 m	2917 m	2862 m
Elevation range	95 m	65 m	63 m	77 m	105 m	94 m	81 m	192 m
Mean aspect	East	South-east	East	North-east	East	East	East	East
Mean slope	12.4°	13.2°	8°	12.5°	10.7°	18.3°	23.5°	25.1°
Area (Ha) in 2011	8.54	4.71	4.74	4.22	7.9	7.35	2.7	5.12
Weighting (since 2011)	0.18	0.11	0.11	0.11	0.16	0.16	0.06	0.11

Title Page

Abstract

Introduction

Conclusions

References

Tables

Figures

◀

▶

◀

▶

Back

Close

Full Screen / Esc

Printer-friendly Version

Interactive Discussion

Evolution of Ossoue Glacier (French Pyrenees) since the end of the Little Ice Age

R. Marti et al.

Title Page

Abstract

Introduction

Conclusions

References

Tables

Figures

◀

▶

◀

▶

Back

Close

Full Screen / Esc

Printer-friendly Version

Interactive Discussion



Table 5. Errors in field measurements at specific sites for winter and annual mass balance measurements, based on estimations by Gerbaux et al. (2005). In the case of Ossoue Glacier, we have considered the entire glacier as an ablation zone, which explains the null value associated with the determination of the transition between two consecutive years.

b_w measurements	Errors (in m w.e.)
Determination of surface level	0.1
Determination of transition between two consecutive years	0
Density measurements	0.05
Snow probing	0.2
<hr/>	
Total in b_w measurements	0.35 m w.e.
<hr/>	
$b_{glac.a}$ measurements	Errors (in m w.e.)
Stake emergence measure	0.04
Determination of surface level	0.1
Density measurement	0.01
<hr/>	
Total in $b_{glac.a}$ measurements ($\sigma_{glac.point}$)	0.15 m w.e.

Evolution of Ossoue Glacier (French Pyrenees) since the end of the Little Ice Age

R. Marti et al.

Table 6. Annualized threshold values to classify the change in intensity of glaciers indicators. The terms $\sigma_{\text{len.a}}$, $\sigma_{\text{area.a}}$, $\sigma_{\text{VR.a}}$, $\sigma_{\text{geod.a}}$, and $\sigma_{\text{gla.a}}$ refer to the annualized random error calculated for each glacier indicator and each period.

Indicators	Marked Negative	Negative	variations		
			No	Positive	Marked Positive
Length	≤ -10 m	$] -10; -\sigma_{\text{len.a}}]$	$\pm\sigma_{\text{len.a}}$	$[+\sigma_{\text{len.a}}; 10[$	≥ 10 m
Area	≤ -1 ha	$] -1; -\sigma_{\text{area.a}}]$	$\pm\sigma_{\text{area.a}}$	$[+\sigma_{\text{area.a}}; 1[$	≥ 1 ha
Elevation change at Villa Russell	≤ -3 m	$] -3; -\sigma_{\text{VR.a}}]$	$\pm\sigma_{\text{VR.a}}$	$[+\sigma_{\text{VR.a}}; 3[$	≥ 3 m
$B_{\text{geod.a}}$	≤ -1 m w.e.	$] -1; -\sigma_{\text{geod.total.a}}]$	$\pm\sigma_{\text{geod.total.a}}$	$[+\sigma_{\text{geod.total.a}}; 1[$	≥ 1 m w.e.
$B_{\text{glac.a}}$	≤ -1 m w.e.	$] -1; -\sigma_{\text{gla.total.a}}]$	$\pm\sigma_{\text{gla.total.a}}$	$[+\sigma_{\text{gla.total.a}}; 1[$	≥ 1 m w.e.

Title Page

Abstract

Introduction

Conclusions

References

Tables

Figures

◀

▶

◀

▶

Back

Close

Full Screen / Esc

Printer-friendly Version

Interactive Discussion



Table 9. Height variations (m) at Ossoue Glacier between the Villa Russell cave threshold and the glacier surface.

Year	Height (m)	Height variation (m)	Annualized variation (m yr^{-1})	Annualized error $\sigma_{\text{VR,a}}$ (m yr^{-1})
1881-82	0	0	0	1.1
1883	-3.5	-3.5	-3.5	1.1
1884	0	3.5	3.5	1.1
1885	1	1	1.0	1.1
1886	4	3	3.0	1.1
1887	6	2	2.0	1.1
1888	0	-6	-6.0	1.1
1889	6	6	6.0	1.1
1890-91-92-93-94	6	0	0	1.1
1895	0	-6	-6.0	1.1
1898	-11	-11	-3.7	0.4
1901	-1.5	9.5	3.2	0.3
1902	-3.5	-2	-2.0	0.7
1904-05	-4.5	-1	-0.5	0.4
1906	-3.75	0.25	0.3	0.7
1907-08	4	7.75	7.8	0.7
1909-10	6	2	2.0	0.7
1911	4	-2	-2.0	0.7
1913	5.5	1.5	0.8	0.4
1927	0.2	-5.3	-0.4	0.1
1937	-3	-3.2	-0.3	0.1
1945	-12	-9	-1.1	0.1
1950	-13.5	-1.5	-0.3	0.1
1952	-2	11.5	5.8	0.4
1953	0	2	2.0	0.7
1967	2	2	0.1	0.1
1983	-0.3	-2.3	-0.1	0.1
1985	-3.6	-3.3	-1.7	0.4
1986	-5	-1.4	-1.4	0.7
1987	-8	-3	-3.0	0.7
1991	-1	7	1.8	0.2
2002	-7	-6	-0.5	0.1
2003	-7.9	-0.9	-0.9	0.7
2004-05	-7.5	0.4	0.4	0.7
2006	-7.3	0.3	0.3	0.7
2007	-11.3	-4	-4.0	0.7
2008	-6.9	4.4	4.4	0.7
2009	-7.5	-0.6	-0.6	0.7
2010	-10.2	-2.7	-2.7	0.7
2011	-14	-3.8	-3.8	0.7
2012	-16.5	-2.5	-2.5	0.7
2013	-12.2	4.3	4.3	0.7

Evolution of Ossoue Glacier (French Pyrenees) since the end of the Little Ice Age

R. Marti et al.

Title Page

Abstract

Introduction

Conclusions

References

Tables

Figures

◀

▶

◀

▶

Back

Close

Full Screen / Esc

Printer-friendly Version

Interactive Discussion



Evolution of Ossoue Glacier (French Pyrenees) since the end of the Little Ice Age

R. Marti et al.

Table 10. Ossoue Glacier volumetric changes: total ice volume variation (ΔV_{ice} in km^3) and associated mass changes in m.w.e. ($d = 900 \text{ kg m}^{-3}$ except for 1948–1983 where $d = 850 \text{ kg m}^{-3}$) for an elementary ice-column. $B_{\text{geod.gla}}$ and $B_{\text{geod.marg}}$ indicate the geodetic mass balance on the glacier and on the margin, respectively. The last columns refer to the annualized rate and annualized systematic and random errors.

Period (years)	ΔV_{ice}	$B_{\text{geod.gla}}$	$B_{\text{geod.marg}}$	$B_{\text{geod.error}}$	Annualized rate	$\overline{\epsilon}_{\text{geod.total.a}}$	$\overline{\sigma}_{\text{geod.total.a}}$
1924–1948 (24)	-0.0324 km^3	-33.5 m.w.e.	-25.5 m.w.e.	8.8 m.w.e.	$-1.39 \text{ m.w.e. yr}^{-1}$	$0.11 + \frac{\epsilon_{\text{bias.1924}}}{24} \text{ m.w.e.}$	0.4 m.w.e.
1948–1983 (35)	$+0.0044 \text{ km}^3$	+5.5 m.w.e.	-7.9 m.w.e.	2.6 m.w.e.	$+0.16 \text{ m.w.e. yr}^{-1}$	0.06 m.w.e.	0.07 m.w.e.
1983–2013 (30)	-0.0219 km^3	-30.1 m.w.e.	-20.3 m.w.e.	1.7 m.w.e.	$-1 \text{ m.w.e. yr}^{-1}$	0.05 m.w.e.	0.05 m.w.e.

Title Page

Abstract

Introduction

Conclusions

References

Tables

Figures

◀

▶

◀

▶

Back

Close

Full Screen / Esc

Printer-friendly Version

Interactive Discussion

Evolution of Ossoue Glacier (French Pyrenees) since the end of the Little Ice Age

R. Marti et al.

Table 11. Ossoue Glacier mass balance time series measured by glaciological methods (in m.w.e.). Annual error based on field measurements is estimated to be 0.15 m.w.e. End_w and End_s refer to the end of winter and the end of summer, respectively, in the floating date system (Cogley et al., 2011). $B_{glac.c}$ means cumulative glaciological mass balances.

	2002	2003	2004	2005	2006	2007	2008	2009	2010	2011	2012	2013	Mean
End_w	30 May	6 Jun.	29 May	28 May	25 May	25 May	6 Jun	30 May	29 May	28 May	26 May	7 Jun	–
End_s	3 Oct	27 Sep	10 Oct	25 Sep	8 Oct	20 Oct	12 Oct	12 Oct	9 Oct	9 Oct	14 Oct	6 Oct	–
B_w	2.09	3.23	3.55	2.58	1.95	2.66	3.24	3.15	3.01	2.12	2.36	3.79	2.81
B_s	–2.93	–4.11	–4.77	–5.07	–4.66	–4.04	–3.35	–4.78	–3.47	–4.56	–5.78	–3.57	–4.26
$B_{glac.a}$	–0.85	–0.88	–1.22	–2.49	–2.71	–1.38	–0.12	–1.63	–0.46	–2.44	–3.42	0.23	–1.45
$B_{glac.c}$	–0.85	–1.73	–2.95	–5.44	–8.15	–9.53	–9.65	–11.27	–11.73	–14.17	–17.59	–17.36	

Title Page

Abstract

Introduction

Conclusions

References

Tables

Figures

◀

▶

◀

▶

Back

Close

Full Screen / Esc

Printer-friendly Version

Interactive Discussion

Evolution of Ossoue Glacier (French Pyrenees) since the end of the Little Ice Age

R. Marti et al.

Title Page

Abstract

Introduction

Conclusions

References

Tables

Figures

◀

▶

◀

▶

Back

Close

Full Screen / Esc

Printer-friendly Version

Interactive Discussion



Table 12. Correlation matrix (Spearman’s ρ_s) between the meteorological time series and the Ossoue Glacier mass balances components (calculated in a fixed date system, Cogley et al., 2011). Correlation values given in parenthesis are based on the monthly mean values. Significant correlations (p values < 0.05) are marked with asterisks. The Gavarnie time series was not complete enough to perform the correlations between the annual mass balance and the annual mean temperature and precipitation over 2002–2011; we reported a no data value (ND) in these cases.

Variables Period of record	$B_{\text{glac.a.1 Oct}}$ mass balance 2002–2013	$B_{\text{s.1 Oct}}$ mass balance 2002–2013	$B_{\text{w.31 May}}$ mass balance 2002–2013	Gavarnie 1992–2012	Pic du Midi temperature 1882–2013	CRU 1858–2013	Gavarnie precipitation 1992–2012	Tarbes precipitation 1882–2012
$B_{\text{glac.a.1 Oct}}$	1	0.84*	0.65*	ND	−0.45	−0.74*	ND	0.66*
$B_{\text{s.1 Oct}}$		1	0.2	−0.72* (−0.81*)	−0.52 (−0.74*)	−0.66 (−0.8*)	–	–
$B_{\text{w.31 May}}$			1	ND	−0.35	0.19	0.71*	0.69*

Evolution of Ossoue Glacier (French Pyrenees) since the end of the Little Ice Age

R. Marti et al.

Title Page

Abstract

Introduction

Conclusions

References

Tables

Figures

◀

▶

◀

▶

Back

Close

Full Screen / Esc

Printer-friendly Version

Interactive Discussion

Table 13. Trends extracted from correlations between temperature and precipitation time series and time (Spearman's ρ). Time structure is based on the interpretation of the glaciological indicators (Fig. 10). Significant correlations (p values < 0.05) are marked with asterisks.

Time structure	Period	ρ_s mean temperature	Mean temperature	ρ_s precipitation	Mean precipitation
1858–1890 (T) 1882–1890 (P)	hydrological year	−0.62*	−1.37 °C	0.25	1219.2 mm
	winter	–	–	0.17	577.8 mm
	summer	−0.36	5.3 °C	–	–
1890–1904	h. year	0.09	−1.3 °C	−0.07	1098 mm
	w.	–	–	−0.11	548.4 mm
	s.	0.14	4.8 °C	–	–
1905–1927	h. year	0.43	−1.6 °C	−0.42	1102.8 mm
	w.	–	–	−0.05	556.2 mm
	s.	0.15	4.3 °C	–	–
1928–1949	h. year	0.29	−1.2 °C	−0.2	993.6 mm
	w.	–	–	−0.19	492.6 mm
	s.	0.26	5.1 °C	–	–
1950–1982	h. year	0.16	−1.4 °C	0.42*	1068 mm
	w.	–	–	0.29	586.2 mm
	s.	0.1	4.8 °C	–	–
1983–2013	h. year	0.38*	−0.4 °C	−0.12	1041.6 mm
	w.	–	–	−0.15	567 mm
	s.	0.43*	6.1 °C	–	–

Evolution of Ossoue Glacier (French Pyrenees) since the end of the Little Ice Age

R. Marti et al.

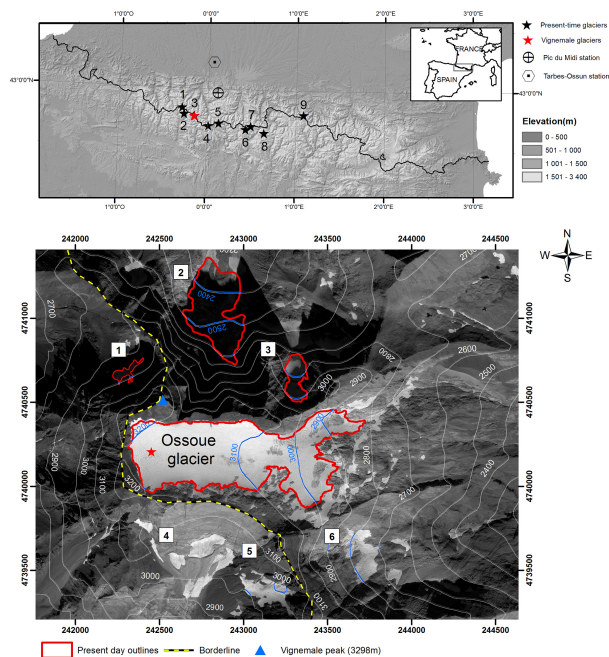


Figure 1. Top: Distribution of the present-day Pyrenean glaciers by mountain massifs: 1. Balaitous; 2. Infierno; 3. Vignemale; 4. Gavarnie-Monte-Perdido; 5. Munia; 6. Posets; 7. Perdiguère; 8. Aneto; 9. Mont-Valier. Bottom: Vignemale Glacieret: 1. Clo de la Hount. Glaciers: 2. Oulettes du Gaube; 3. Petit-Vignemale and Ossoue. Vanished glaciers: 4. Spanish Monferrat; 5. Tapou; 6. French Montferrat. We note that the vanished glaciers were oriented to the southwest and east. Clo de la Hount is northwest-oriented and its area is less than 0.01 km^2 (2011). North-oriented glaciers Oulettes du Gaube, 0.13 km^2 (2011), and Petit Vignemale, 0.03 km^2 (2011), were one unique glacier until 1888 (Reid-Muret, 1906). Coordinate system: UTM 31° N .

Title Page

Abstract

Introduction

Conclusions

References

Tables

Figures

◀

▶

◀

▶

Back

Close

Full Screen / Esc

Printer-friendly Version

Interactive Discussion

Evolution of Ossoue Glacier (French Pyrenees) since the end of the Little Ice Age

R. Marti et al.



Figure 2. Photo-comparison of Ossoue Glacier (Vignemale Massif): left, 1911 (Gaurier L.); right, 2011 (René P.).

Title Page

Abstract

Introduction

Conclusions

References

Tables

Figures

◀

▶

◀

▶

Back

Close

Full Screen / Esc

Printer-friendly Version

Interactive Discussion

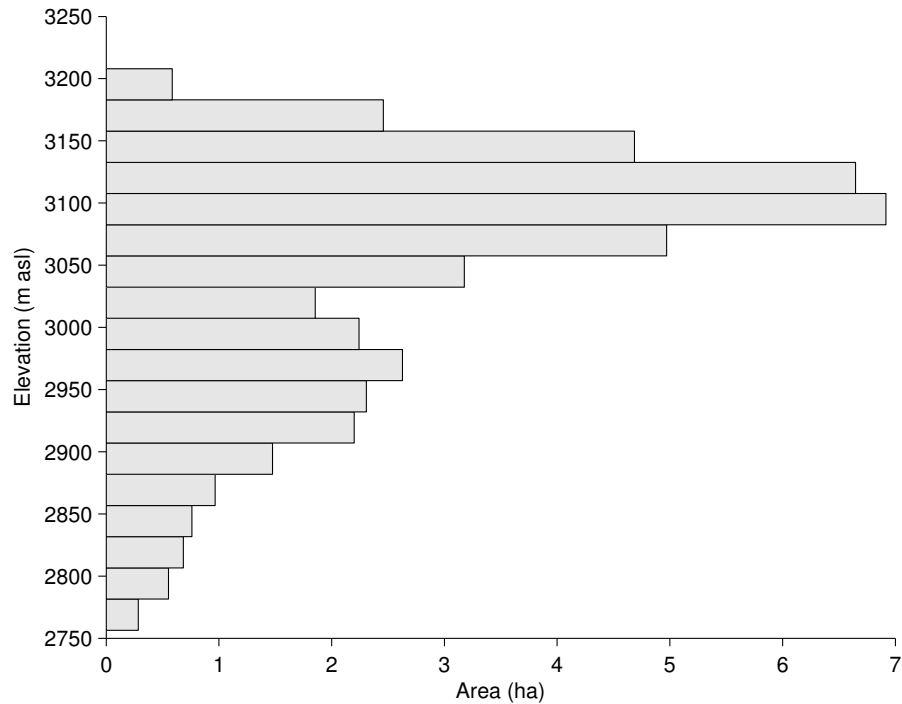


Figure 3. Ossoue Glacier hypsography in 25 m bins (2013).

Evolution of Ossoue Glacier (French Pyrenees) since the end of the Little Ice Age

R. Marti et al.

[Title Page](#)

[Abstract](#) | [Introduction](#)

[Conclusions](#) | [References](#)

[Tables](#) | [Figures](#)

[◀](#) | [▶](#)

[◀](#) | [▶](#)

[Back](#) | [Close](#)

[Full Screen / Esc](#)

[Printer-friendly Version](#)

[Interactive Discussion](#)



Evolution of Ossoue Glacier (French Pyrenees) since the end of the Little Ice Age

R. Marti et al.

Title Page

Abstract

Introduction

Conclusions

References

Tables

Figures

◀

▶

◀

▶

Back

Close

Full Screen / Esc

Printer-friendly Version

Interactive Discussion

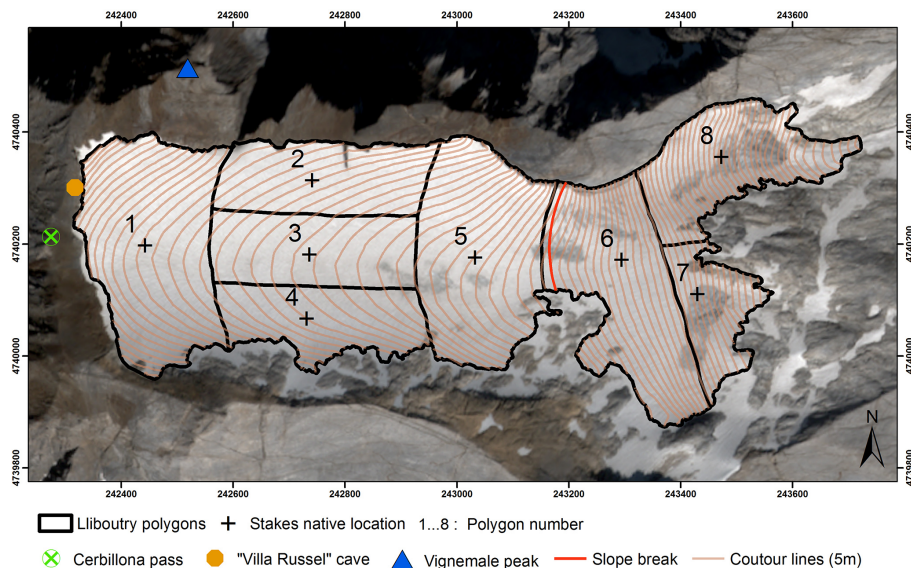


Figure 4. Distribution of stakes at Ossoue Glacier. CNES©image Pléiades MS-09-23-2013. UTM 31° N projection.

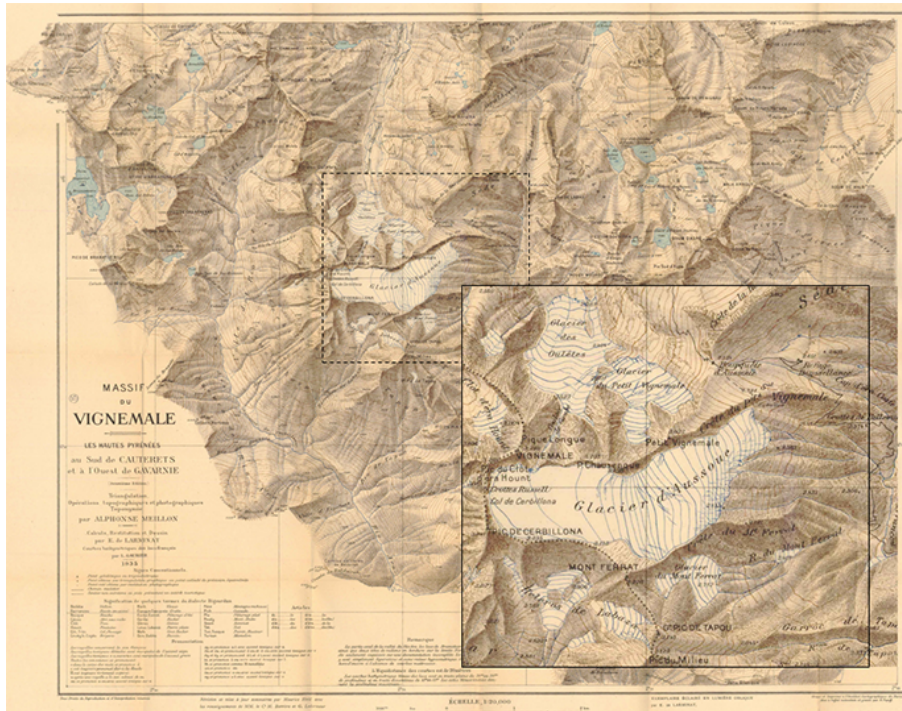


Figure 5. Map designed by Meillon and Larminat, with focus on Vignemale Glaciers, 1933 edition (Glacier data are from 1924).

Evolution of Ossoue Glacier (French Pyrenees) since the end of the Little Ice Age

R. Marti et al.

Title Page

Abstract Introduction

Conclusions References

Tables Figures

◀ ▶

◀ ▶

Back Close

Full Screen / Esc

Printer-friendly Version

Interactive Discussion



Evolution of Ossoue Glacier (French Pyrenees) since the end of the Little Ice Age

R. Marti et al.

Title Page

Abstract

Introduction

Conclusions

References

Tables

Figures

◀

▶

◀

▶

Back

Close

Full Screen / Esc

Printer-friendly Version

Interactive Discussion

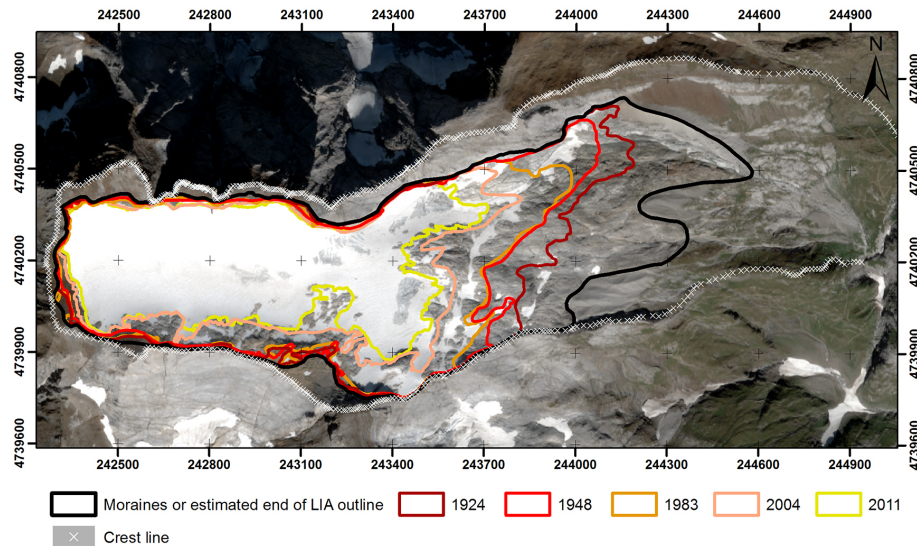


Figure 6. Evolution of Ossoue Glacier area since the LIA. The glacier outlines are superposed on a multispectral Pléiades ortho-image taken on 23 September 2013. UTM 31° N projection.

Evolution of Ossoue Glacier (French Pyrenees) since the end of the Little Ice Age

R. Marti et al.

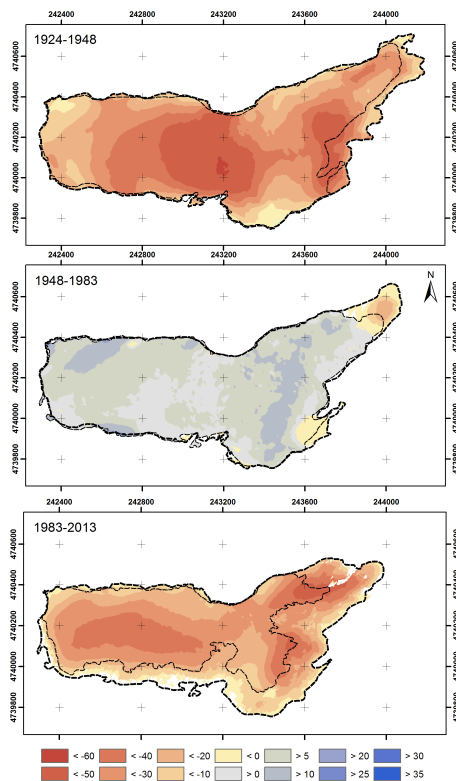


Figure 7. Elevations differences (m) on glacier (thin dashed line) and on deglaciated margins (thick dashed line) based on differences between consecutive DEMs. UTM 31° N projection.

Title Page

Abstract

Introduction

Conclusions

References

Tables

Figures

◀

▶

◀

▶

Back

Close

Full Screen / Esc

Printer-friendly Version

Interactive Discussion

Evolution of Ossoue Glacier (French Pyrenees) since the end of the Little Ice Age

R. Marti et al.

Title Page

Abstract

Introduction

Conclusions

References

Tables

Figures

◀

▶

◀

▶

Back

Close

Full Screen / Esc

Printer-friendly Version

Interactive Discussion

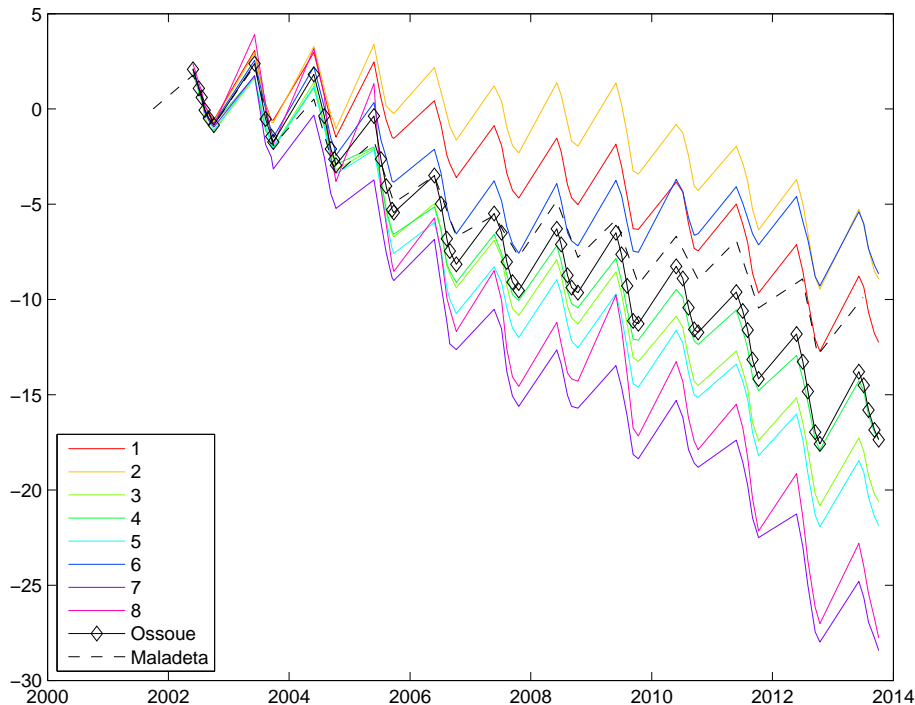


Figure 8. Glacier surface elevation variations in m.w.e. at Ossoue stake locations from 2001 to 2013. For details of stake locations on the glacier, see Fig. 4 and Tab. 4. Maladeta Glacier is indicated by the dashed gray line.

Evolution of Ossoue Glacier (French Pyrenees) since the end of the Little Ice Age

R. Marti et al.

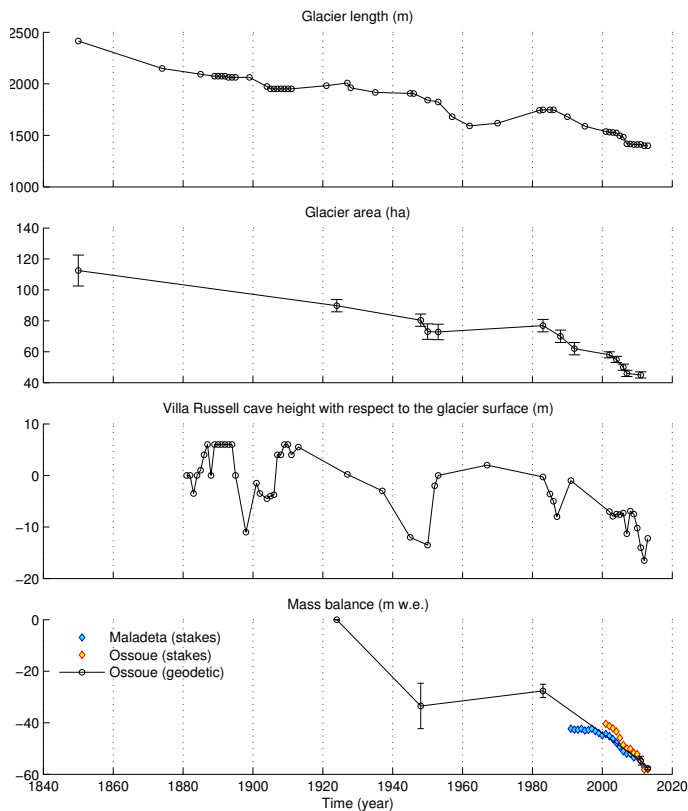


Figure 9. Length (m), area (ha) and thickness (m) at Villa Russell and volumetric mass changes (in m w.e.) of Ossoue Glacier. Glaciological mass balances of Ossoue (orange) and Maladeta (blue) Glaciers.

Title Page

Abstract Introduction

Conclusions References

Tables Figures

◀ ▶

◀ ▶

Back Close

Full Screen / Esc

Printer-friendly Version

Interactive Discussion



Evolution of Ossoue Glacier (French Pyrenees) since the end of the Little Ice Age

R. Marti et al.

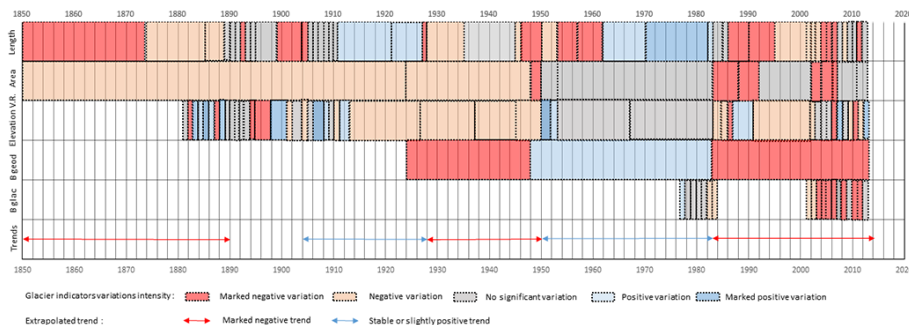


Figure 10. Qualitative changes of Ossoue Glacier indicators based on annual threshold values (Tab. 6): length, area, and thickness at Villa Russell, B_{geod} , B_{glacio} and interpreted trends from the combination of indicators.

Title Page

Abstract

Introduction

Conclusions

References

Tables

Figures

◀

▶

◀

▶

Back

Close

Full Screen / Esc

Printer-friendly Version

Interactive Discussion

Evolution of Ossoue Glacier (French Pyrenees) since the end of the Little Ice Age

R. Marti et al.

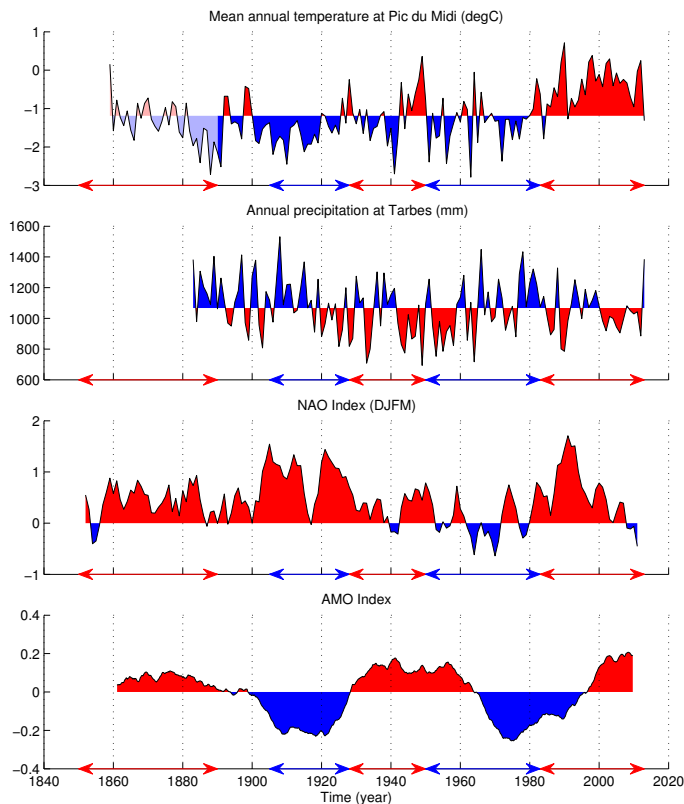


Figure 11. Climatic time series: mean annual temperature at Pic du Midi (beginning 1 October), annual precipitation at Tarbes, AMO mode and winter NAO (DJFM) anomalies. Double arrows on the time line are reported from the glacier fluctuations (blue: stable or positive trend, red: marked negative trend) identified by the combination of glacier indicators.

[Title Page](#)
[Abstract](#)
[Introduction](#)
[Conclusions](#)
[References](#)
[Tables](#)
[Figures](#)
[◀](#)
[▶](#)
[◀](#)
[▶](#)
[Back](#)
[Close](#)
[Full Screen / Esc](#)
[Printer-friendly Version](#)
[Interactive Discussion](#)

Evolution of Ossoue Glacier (French Pyrenees) since the end of the Little Ice Age

R. Marti et al.

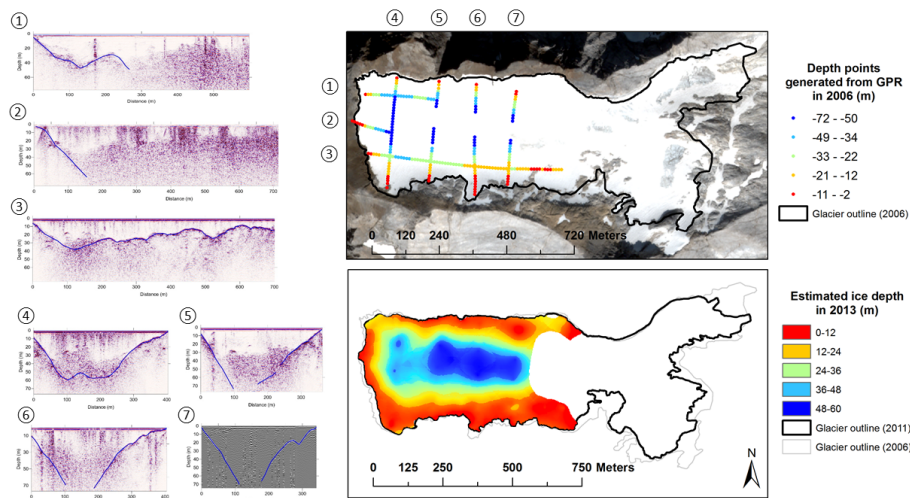


Figure 12. Map: Bedrock depth as interpreted from GPR radargrams plotted atop a 2013 XS Pléiades image. Numbers 1 to 3: interpretations of longitudinal radargram acquisitions. Numbers 4 to 7: interpretations of transverse radargram acquisitions.

Title Page

Abstract Introduction

Conclusions References

Tables Figures

◀ ▶

◀ ▶

Back Close

Full Screen / Esc

Printer-friendly Version

Interactive Discussion

